



**NAVAL
POSTGRADUATE
SCHOOL**

MONTEREY, CALIFORNIA

THESIS

**INITIAL INVESTIGATION OF A NOVEL THERMAL
STORAGE CONCEPT AS PART OF A RENEWABLE
ENERGY SYSTEM**

by

Lindsay M. Olsen

June 2013

Thesis Advisor:
Co-Advisor:

Anthony J. Gannon
Garth V. Hobson

Approved for public release; distribution is unlimited

THIS PAGE INTENTIONALLY LEFT BLANK

REPORT DOCUMENTATION PAGE			<i>Form Approved OMB No. 0704-0188</i>	
Public reporting burden for this collection of information is estimated to average 1 hour per response, including the time for reviewing instruction, searching existing data sources, gathering and maintaining the data needed, and completing and reviewing the collection of information. Send comments regarding this burden estimate or any other aspect of this collection of information, including suggestions for reducing this burden, to Washington headquarters Services, Directorate for Information Operations and Reports, 1215 Jefferson Davis Highway, Suite 1204, Arlington, VA 22202-4302, and to the Office of Management and Budget, Paperwork Reduction Project (0704-0188) Washington DC 20503.				
1. AGENCY USE ONLY (Leave blank)		2. REPORT DATE June 2013	3. REPORT TYPE AND DATES COVERED Master's Thesis	
4. TITLE AND SUBTITLE INITIAL INVESTIGATION OF A NOVEL THERMAL STORAGE CONCEPT AS PART OF A RENEWABLE ENERGY SYSTEM			5. FUNDING NUMBERS	
6. AUTHOR(S) Lindsay M. Olsen			8. PERFORMING ORGANIZATION REPORT NUMBER	
7. PERFORMING ORGANIZATION NAME(S) AND ADDRESS(ES) Naval Postgraduate School Monterey, CA 93943-5000			10. SPONSORING/MONITORING AGENCY REPORT NUMBER	
9. SPONSORING /MONITORING AGENCY NAME(S) AND ADDRESS(ES) N/A			11. SUPPLEMENTARY NOTES The views expressed in this thesis are those of the author and do not reflect the official policy or position of the Department of Defense or the U.S. Government. IRB Protocol number ___N/A___.	
12a. DISTRIBUTION / AVAILABILITY STATEMENT Approved for public release; distribution is unlimited			12b. DISTRIBUTION CODE	
13. ABSTRACT (maximum 200 words) This thesis forms part of a larger study that aims to develop a renewable energy demonstration plant at the Naval Postgraduate School Turbopropulsion Laboratory. The architecture and design approach of the demonstration plant is outlined in this thesis. While all the components of the system are commercially available, the integration of the components is challenging. The results of the design approach presented the optimal way of integrating wind turbines, an electrical system, chiller units, and thermal storage tanks. Modular ice thermal tanks with polypropylene tubing were chosen for storage. The ice thermal storage units were selected over battery storage as they are more cost effective and potentially safer. A statistical analysis was performed using wind data from Monterey Airport, which was beneficial for choosing which wind turbines to implement in the system. The analysis determined that total energy captured by two, 4-kW vertical axis wind turbines was 2,554.8 kW-hours annually. Additionally, ANSYS Fluent was used to analyze the ice growth around the tubing at various ice and tube thicknesses. The ANSYS Fluent analysis showed that ice thickness affects the ice volume growth and change in enthalpy change more than wall thickness affects these conditions.				
14. SUBJECT TERMS Renewable energy, thermal ice storage, chiller, cooling, wind energy			15. NUMBER OF PAGES 91	
			16. PRICE CODE	
17. SECURITY CLASSIFICATION OF REPORT Unclassified	18. SECURITY CLASSIFICATION OF THIS PAGE Unclassified	19. SECURITY CLASSIFICATION OF ABSTRACT Unclassified	20. LIMITATION OF ABSTRACT UU	

THIS PAGE INTENTIONALLY LEFT BLANK

Approved for public release; distribution is unlimited

**INITIAL INVESTIGATION OF A NOVEL THERMAL STORAGE CONCEPT
AS PART OF A RENEWABLE ENERGY SYSTEM**

Lindsay M. Olsen
Ensign, United States Navy
B.S., United States Naval Academy, 2012

Submitted in partial fulfillment of the
requirements for the degree of

MASTER OF SCIENCE IN MECHANICAL ENGINEERING

from the

**NAVAL POSTGRADUATE SCHOOL
June 2013**

Author: Lindsay M. Olsen

Approved by: Anthony J. Gannon
Thesis Advisor

Garth V. Hobson
Thesis Co-Advisor

Knox T. Millsaps
Chair, Department of Mechanical and Aerospace Engineering

THIS PAGE INTENTIONALLY LEFT BLANK

ABSTRACT

This thesis forms part of a larger study that aims to develop a renewable energy demonstration plant at the Naval Postgraduate School Turbopropulsion Laboratory. The architecture and design approach of the demonstration plant is outlined in this thesis. While all the components of the system are commercially available, the integration of the components is challenging. The results of the design approach presented the optimal way of integrating wind turbines, an electrical system, chiller units, and thermal storage tanks. Modular ice thermal tanks with polypropylene tubing were chosen for storage. The ice thermal storage units were selected over battery storage as they are more cost effective and potentially safer.

A statistical analysis was performed using wind data from Monterey Airport, which was beneficial for choosing which wind turbines to implement in the system. The analysis determined that total energy captured by two, 4-kW vertical axis wind turbines was 2,554.8 kW-hours annually. Additionally, ANSYS Fluent was used to analyze the ice growth around the tubing at various ice and tube thicknesses. The ANSYS Fluent analysis showed that ice thickness affects the ice volume growth and change in enthalpy change more than wall thickness affects these conditions.

THIS PAGE INTENTIONALLY LEFT BLANK

TABLE OF CONTENTS

I.	INTRODUCTION.....	1
A.	RENEWABLE ENERGY	1
1.	Legacy Renewables	2
2.	End-Use Renewables.....	2
a.	<i>Batteries</i>.....	2
b.	<i>Thermal Storage</i>.....	3
B.	MILITARY APPLICATIONS	4
1.	Operational.....	4
2.	Economic.....	6
3.	Environmental.....	7
4.	“Net-zero” Installations.....	7
5.	Energy System Technology Evaluation Program	7
C.	PROJECT OBJECTIVES.....	8
D.	LITERATURE REVIEW	9
II.	SYSTEM ANALYSIS.....	11
A.	STATISTICAL ANALYSIS OF WIND DATA	11
B.	POWER CURVES	12
III.	PLANT ARCHITECTURE	17
A.	WIND TURBINE AND WINDY BOY INVERTERS	20
B.	CHILLER SYSTEM AND THERMAL ENERGY STORAGE.....	21
C.	STABILITY BATTERY, GRID-CONNECTION, AND SMA SUNNY ISLAND	23
IV.	SOLIDIFICATION MODELING.....	25
A.	INTRODUCTION.....	25
B.	MODELING THE SYSTEM.....	25
C.	RESULTS	31
V.	CONCLUSION	33
VI.	RECOMMENDATIONS.....	35
	APPENDIX A	37
	APPENDIX B	39
	APPENDIX C	43
	APPENDIX D	67
	APPENDIX E	69
	LIST OF REFERENCES	71
	INITIAL DISTRIBUTION LIST	73

THIS PAGE INTENTIONALLY LEFT BLANK

LIST OF FIGURES

Figure 1.	Renewable Energy as Share of Total Primary Energy Consumption. From [1].	1
Figure 2.	Gravimetric energy density versus volumetric energy density. After [5].	4
Figure 3.	Proven conventional oil reserves (2008). From [8].	5
Figure 4.	U.S. total annual casualties in OEF versus U.S. fuel consumed. From [8].	6
Figure 5.	Energy usage breakdown in commercial spaces in 2005. From [13].	9
Figure 6.	Wind Rose: Monterey, CA January 1998-August 2012.	12
Figure 7.	Wind velocity vs. year.	13
Figure 8.	CDF plot of wind velocity.	14
Figure 9.	Power output vs. wind speed. From [19].	15
Figure 10.	Power vs. time.	15
Figure 11.	Typical cooling schematic.	17
Figure 12.	Proposed demonstration plant schematic.	18
Figure 13.	Google Maps image of NPS Turbopropulsion Laboratory.	19
Figure 14.	SolidWorks model of NPS Turbopropulsion Laboratory, including electrical system, chiller, and thermal storage tanks.	20
Figure 15.	Urban Green Energy 4 kW Vertical Axis Turbine. From [19].	21
Figure 16.	CALMAC Thermal Energy Storage tanks 1045A. From [20].	22
Figure 17.	Inside of a CALMAC Thermal Energy Storage tank 1045A, with polypropylene tubing. From [20].	22
Figure 18.	Quartered section of thermal ice storage system tubing.	26
Figure 19.	Quartered section of thermal ice storage system tubing—Detail.	27
Figure 20.	Mesh of quartered tube section.	28
Figure 21.	Sweep and inflation methods of meshing.	29
Figure 22.	Nondimensionalized mass-weighted enthalpy vs. ice thickness.	31
Figure 23.	Volume of ice produced vs. thickness of ice.	32
Figure 24.	Inlet with a tube thickness of 0.0002 m and an ice thickness of 0.0204 m.	39
Figure 25.	Outlet with a tube thickness of 0.0002 m and an ice thickness of 0.0204 m.	40
Figure 26.	Side view of a tube with thickness of 0.0002 m and an ice thickness of 0.0204 m.	41

THIS PAGE INTENTIONALLY LEFT BLANK

LIST OF TABLES

Table 1. Purchase Price of Various Storage Devices per kW-hr. After [4].3

THIS PAGE INTENTIONALLY LEFT BLANK

LIST OF ACRONYMS AND ABBREVIATIONS

AC	Alternating current
CDF	Cumulative Distribution Function
DC	Direct current
DoD	Department of Defense
ESTEP	Energy System Technology Evaluation Program
NPS	Naval Postgraduate School

THIS PAGE INTENTIONALLY LEFT BLANK

ACKNOWLEDGMENTS

First, I would like to offer my sincere appreciation to the faculty and staff at Naval Postgraduate School's Turbopropulsion Laboratory. Dr. Anthony Gannon served as a knowledgeable and interested advisor. His guidance and dedication shaped not only this thesis but also the implementation of the entire demonstration plant. Dr. Garth Hobson's assistance was treasured both in the laboratory and in the classroom. My understanding of computational fluid dynamics, which directly impacted this project, would have been severely weakened without his help. I would also like to thank CDR Scott Drayton for offering his expertise on topics concerning both mechanical engineering and life in the Navy.

I would like to thank Professor Michael Schultz, my Bowman Scholar project advisor at the United States Naval Academy for introducing me to the field of Fluid Mechanics. I learned valuable lessons during my undergraduate research that made this thesis infinitely more successful.

Finally, I would like to thank my family and friends for their support during this process. This thesis would not have been possible without the love and encouragement of my mother, Simone, and my sister, Caitlin. I'd also like to thank my uncle Greg, who has taught me the value of education.

THIS PAGE INTENTIONALLY LEFT BLANK

I. INTRODUCTION

A. RENEWABLE ENERGY

The primary sources of energy in the United States are currently being used at an unsustainable rate. As a result, the U.S. government has committed to increasing the production and use of renewable energy resources. Diversifying the energy infrastructure will enhance energy security while greatly benefiting the environment. Figure 1 shows that 36% of energy consumed in the U.S. in 2011 came from petroleum, with only 9% coming from all renewable energy resources combined.

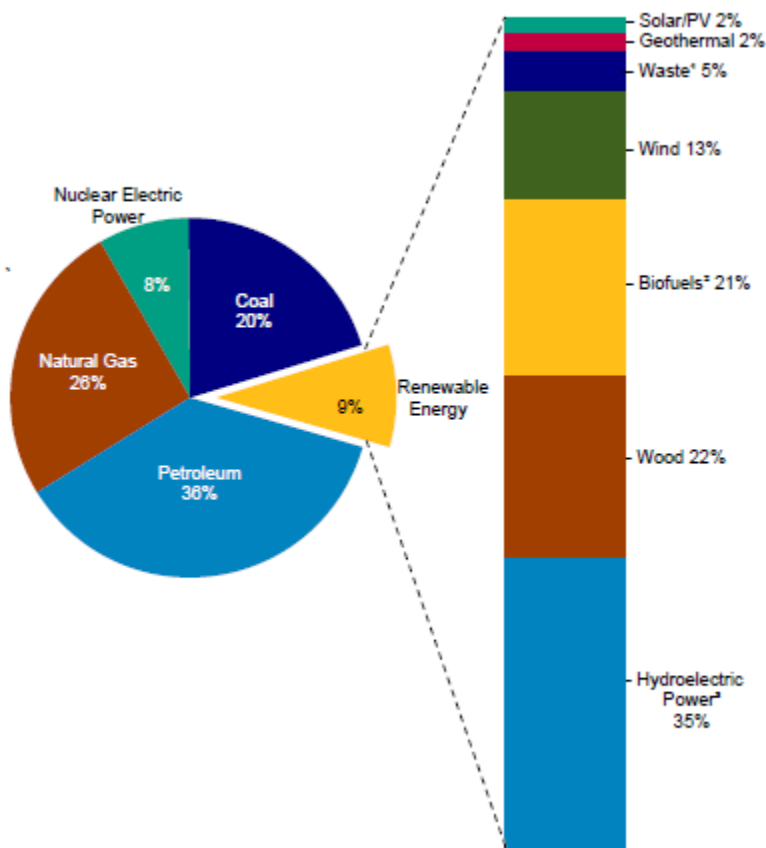


Figure 1. Renewable Energy as Share of Total Primary Energy Consumption. From [1].

The Department of Energy projects that by 2040, 23-31% of electricity used in the U.S. will be from renewable resources [2]. This marked increase indicates the importance of developing renewable energy technology for the future.

1. Legacy Renewables

The term “legacy renewables” is intended to refer to renewable energy technology that has been extensively developed and used. This includes the renewable energy sources that are directly linked to the electrical grid. In the United States, most large-scale wind turbine and solar photovoltaic farms are directly connected to the electrical grid. Both wind and solar are intermittent sources of energy. Wind power output is directly affected by wind conditions and air density, while solar is affected by the season, the time of day, and cloud coverage. To maintain grid stability, instantaneous electrical generation must match consumption. Figure 1 indicates that solar and wind power combined only contributes 1.35% of the total energy consumed in the United States. With these low contribution levels, maintaining grid stability is not difficult. Wind, however, is the fastest growing renewable resource in the United States [1]. Grid stability will be a substantial issue when solar and wind resources become a more significant contributor to the electrical grid. For this reason, off-grid solutions, including the one proposed in this thesis, are becoming especially relevant.

2. End-Use Renewables

“End-use renewables” refer to renewable energy resources in self-contained systems. Batteries are the most common method of storing off-grid power; however, thermal storage systems for heating and cooling applications are a valuable alternative.

a. Batteries

There are a multitude of batteries used for renewable energy storage systems, including nickel-cadmium, lithium-ion, alkaline-cell, and lead-acid batteries. Lead-acid batteries are the most common, comprising 40-45% of batteries sold worldwide [3]. Their popularity is due to their relatively low cost, coupled with a high

electrical efficiency and a high power-density. One major disadvantage of lead-acid batteries is the potential for a hydrogen evolution reaction to occur, which can cause the battery to explode.

b. Thermal Storage

There are numerous methods of thermal storage; however, this thesis will focus on ice-based thermal storage. Heat of fusion refers to the enthalpy change that occurs when a substance changes phase from a solid to a liquid. Ice storage takes advantage of the high heat of fusion of water (334.0 kJ/kg).

There are numerous advantages to using ice storage. Compared to batteries, ice storage is inexpensive. Table 1 indicates that the purchase price of thermal ice storage is approximately one-quarter of that of an alkaline-cell or lead-acid battery and one-tenth of that of a lithium-ion battery.

Thermal ice storage	Alkaline-cell battery	Lead-acid battery	Lithium-ion battery
\$37	\$140	\$150	\$400

Table 1. Purchase Price of Various Storage Devices per kW-hr. After [4].

Thermal ice storage is significantly less hazardous than battery storage. In addition, ice storage does not have a limiting life cycle. Batteries can only be recharged a given number of times, while the ice in thermal storage tanks can freeze and unfreeze for an unlimited number of cycles. Figure 2 shows a plot of gravimetric energy density versus volumetric energy density. This plot shows that the weight to size ratio of an ice storage system is comparable to that of a lead-acid battery.

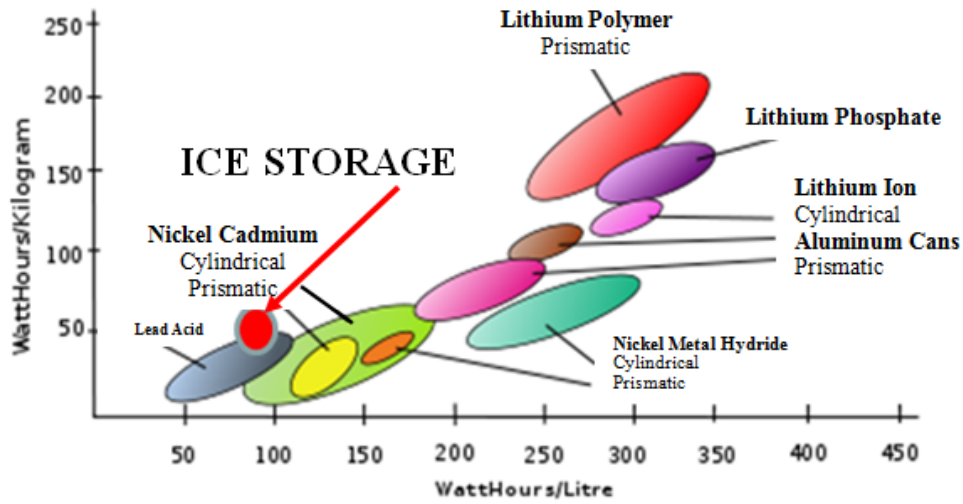


Figure 2. Gravimetric energy density versus volumetric energy density. After [5].

B. MILITARY APPLICATIONS

The Department of Defense is the largest single consumer of energy in the United States. In FY2011, DoD spent \$17 billion on fuel, approximately two-thirds of which came from petroleum-based products [6]. As such, DoD has become proactive about establishing an energy-secure force by both improving energy efficiency and investing in renewable energy. There are operational, economic, and environmental benefits to doing so [7].

1. Operational

There are many operational benefits that come with energy security. The U.S.'s dependence on foreign oil is inextricably tied to national security, and therefore military strategy and procedure. A chart of conventional oil reserves around the globe is shown in Figure 3

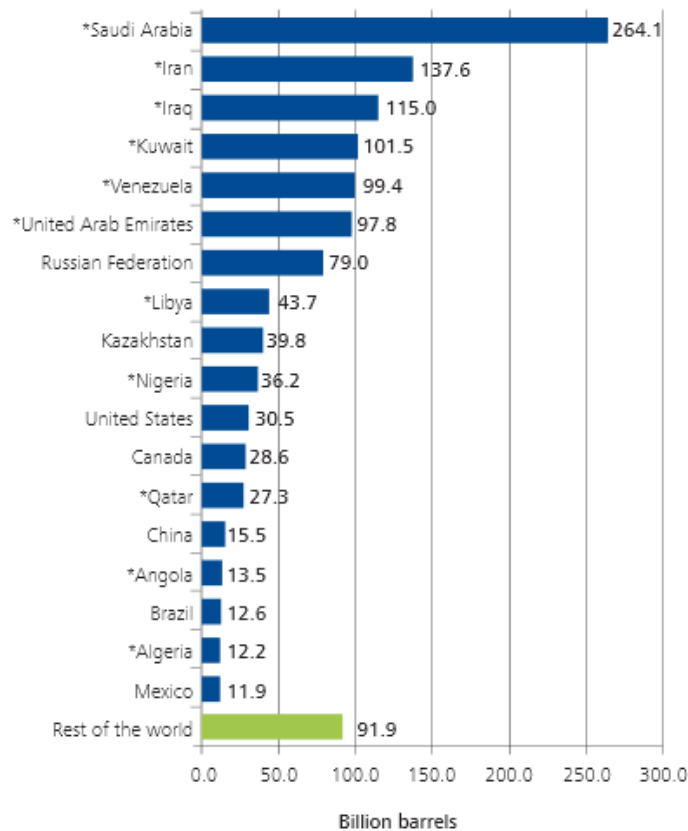


Figure 3. Proven conventional oil reserves (2008). From [8].

Of these nations, only Mexico and Canada are considered “strategically reliable sources of energy to the United States,” [8]. This renders the U.S. extremely vulnerable to the will of strategically unreliable foreign nations. Achieving energy security would lessen the dependence on these foreign nations while improving “the range, endurance, and reliability of ground, air, and naval forces,” [9].

One common strategic benefit of attaining energy security that is frequently cited by military officials is reducing the importance of fuel lines and convoys. A single forward operating base in Afghanistan requires at least 300 gallons of diesel per day [8]. Fuel lines and convoys are essential to providing fuel to these bases, which are spread throughout the country. Convoys are extremely vulnerable to IED attacks, environmental mishaps, and traffic accidents as they travel from base to base. In fact, there is a direct

relationship between the amount of fuel consumed in Afghanistan and troop casualties, as shown in Figure 4.

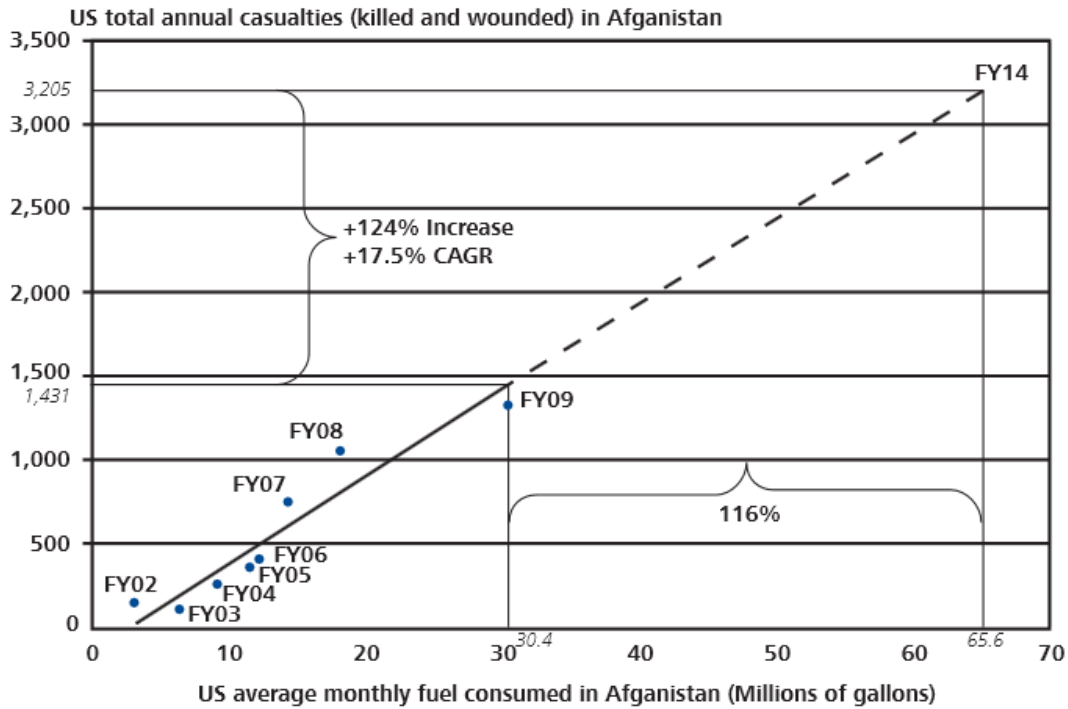


Figure 4. U.S. total annual casualties in OEF versus U.S. fuel consumed. From [8].

Reducing the dependence on petroleum and utilizing other energy resources will greatly simplify the logistics of an operation. With less fuel to be moved, fewer casualties will occur.

2. Economic

As discussed in the “Operational” section, the U.S. is dependent on strategically unreliable foreign nations for fuel import. This makes the DoD vulnerable to fluctuations in availability and price of petroleum. Diversifying its energy supply with renewable resources and becoming more efficient will reduce petroleum demand and increase DoD self-sufficiency during this financially delicate time.

It is also important to note the “fully-burdened” cost of fuel, which accounts for transportation cost of the fuel, as well as the cost of the air and land forces used to

protect it. The Marine Corps estimated that the “fully-burdened” cost of a gallon of fuel ranged from \$9 to \$16 per gallon for land deliveries and from \$29 to \$31 per gallon for air deliveries [10].

3. Environmental

While the main goal of the DoD in becoming energy-secure is to save lives and reduce spending, it is important that military and national policy are in alignment. The DoD’s current energy policy is in agreement with the United States’ energy policy, which emphasizes reducing greenhouse gas emissions and reliance on fossil fuels in order to protect the environment from further damage.

4. “Net-zero” Installations

The ultimate goal of the DoD and the U.S. Department of Energy is to establish “net-zero” energy installations. A “net-zero” site is defined as one that “produces as much energy on-site from renewable energy generation or through the on-site use of renewable fuels, as it consumes in its buildings, facilities, and fleet vehicles” [11]. Wind turbines are one source of renewable energy that is being used to meet this net-zero goal. Currently, wind turbines are being used to provide electricity at a number of military installations, including Guantanamo Bay and San Clemente Island [12]. Typically, these systems implement battery storage, which, as discussed in section I.A.2, can be costly and dangerous. On bases within the United States, battery storage is a reasonably safe and viable option; however, on forward operating bases, especially those within a warzone, having exposed batteries can be extremely hazardous. Using ice as a direct thermal storage method, as this project proposes, has the potential to save fuel and therefore money. In addition, it may be safer in forward-operating areas.

5. Energy System Technology Evaluation Program

The Office of Naval Operations has provided funding to the Energy System Technology Evaluation Program (ESTEP). This program supports both technology- and policy-based projects focusing on various energy-related topics. The projects use Navy and Marine Corps facilities and resources for testing. At NPS, numerous ESTEP-funded

projects are conducted within in the Operations Research and Mechanical and Aerospace Engineering Departments. This project, which focuses on the implementation of a renewable energy-based cooling system, was funded by ESTEP.

C. PROJECT OBJECTIVES

The ultimate goal of this project is to develop a demonstration plant that uses wind to power a commercial chiller unit at the Naval Postgraduate School (NPS) Turbopropulsion Laboratory. The excess cooling will be used to freeze water, which will be stored in a thermal storage unit. Wind power is intermittent, so when the turbines are not spinning and producing power, the ice storage unit will discharge to cool the building. While ice storage has become fairly common for cooling purposes, there has yet to be a system that uses wind or another renewable energy source to power such a system.

Ultimately, this demonstration plant would serve as a model for forward operating bases and remote stations. The ice storage makes the system grid-independent, and in addition, commercial chillers can be readily purchased, transferred to, and set up in international areas. Ideally, a system like this could be used to cool data centers or other spaces in forward-operating bases. Figure 5 shows that space cooling represents 13.1% of energy consumed in commercial spaces in 2005. This indicates the significance of developing renewable energy resources that caters to this application.

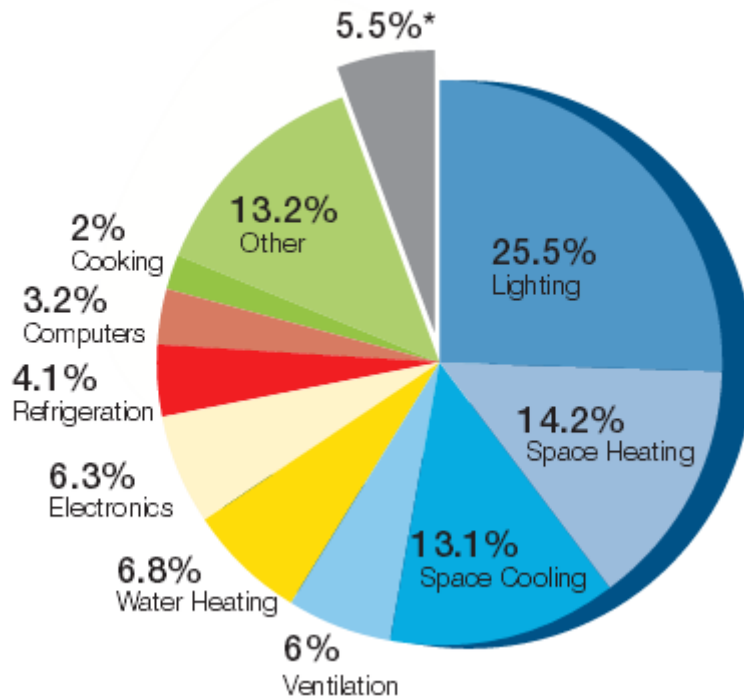


Figure 5. Energy usage breakdown in commercial spaces in 2005. From [13].

This system is in direct accordance with the military’s goal to reduce petroleum usage and to increase the use of renewable energy resources.

D. LITERATURE REVIEW

Although research into thermal energy storage is ongoing, ice storage for cooling has been implemented in various cases, as shown in cases like [14], [15], and [16]. A wind-driven chilling system using ice storage has yet to be developed. Holly Chrystle Davis submitted a graduate thesis that explored wind-electric ice making to the University of Colorado in 1994. A variable-frequency wind generator powered an ice maker, which was used to preserve fish and produce in developing nations. The University of Colorado, the National Renewable Energy Laboratory, and Bergey Windpower Company, Inc. participated in setting up this demonstration plant. Davis showed that a variable-frequency wind turbine *can* operate a conventional ice maker, although she experienced problems with “large start-up currents and corresponding voltage drops that occurred” when an ice maker was turned on [17]. Other than this

small-scale project, a renewable energy powered cooling system using ice thermal storage is a novel idea, and as such, limited research is available.

II. SYSTEM ANALYSIS

The goal of the system analysis was to determine the total energy captured by a wind turbine in one year. To accomplish this, a statistical analysis of wind data was done using MATLAB.

A. STATISTICAL ANALYSIS OF WIND DATA

Weather data statistics, including the wind from the Monterey Airport was obtained from 1980 to August 2012. The data included measurements of the wind speed and direction at various times throughout the day. Before 1998, the wind data was incomplete, with large gaps of missing data. Because the data from 1980-1997 was not complete, it was decided that the information from January 1998 to August 2012 would be used to complete the statistical analysis. The reduced data still yielded 160,706 data points, or an average of 30 points per day. The wind rose in Figure 6 shows the frequency of the wind blowing from a given direction. At the Monterey Airport, which is less than a mile from the NPS Turbopropulsion Laboratory as the crow flies, the prevailing winds come from the west. The average overall wind speed was 5.77 mph, or 2.58 m/s. The median wind speed was 6.00 mph, or 2.68 m/s.

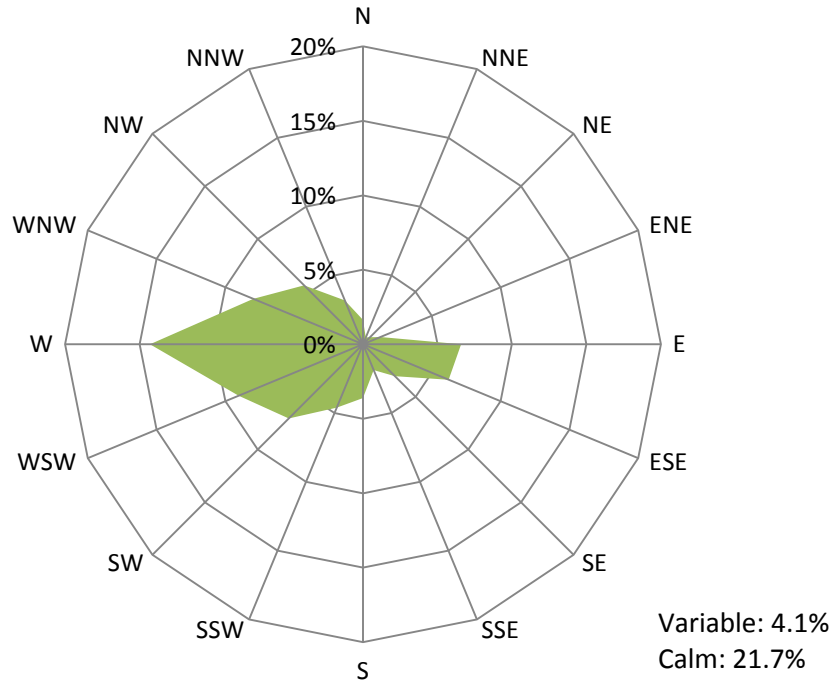


Figure 6. Wind Rose: Monterey, CA January 1998-August 2012.

B. POWER CURVES

A MATLAB analysis of the wind data was subsequently completed. The MATLAB script can be found in Appendix A. The first step in the analysis was to graph the wind velocity vs. the year in MATLAB, as shown in Figure 7.

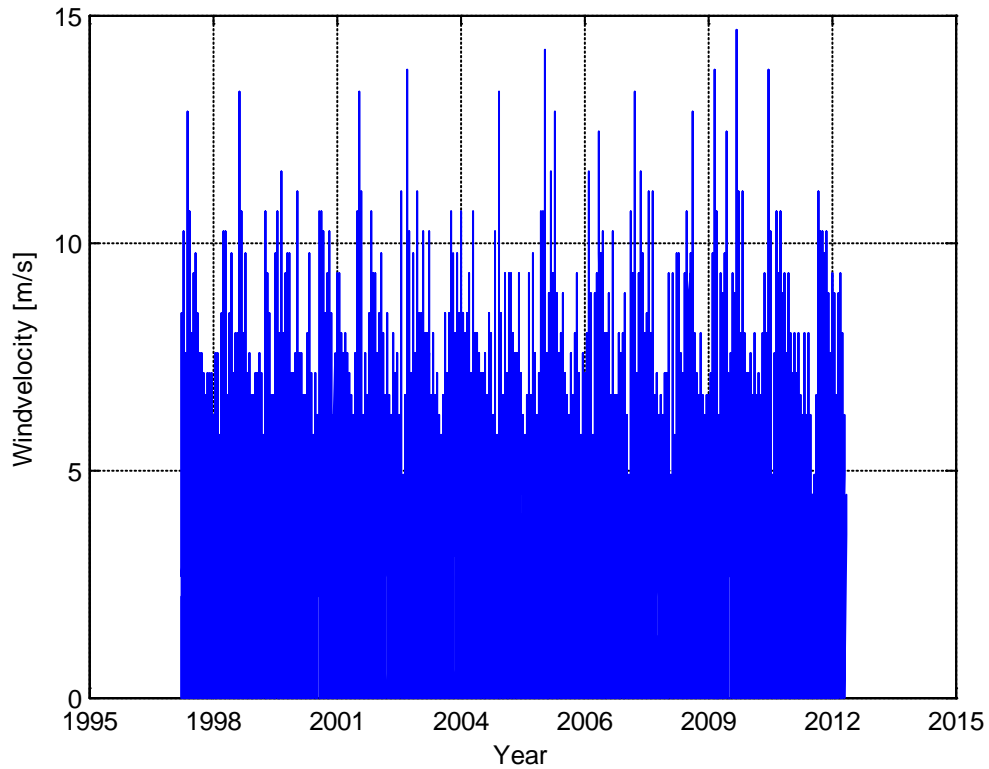


Figure 7. Wind velocity vs. year.

The wind velocity was plotted as a cumulative distribution function (CDF). A CDF is a statistical distribution that describes the probability that a random variable is less than or equal to the independent variable of the function. This graph, shown in Figure 8, serves as a useful first step in determining the wind characteristics of a given site. Once the wind characteristics are determined, an appropriate turbine can be chosen. This process was detailed by Taylor [18].

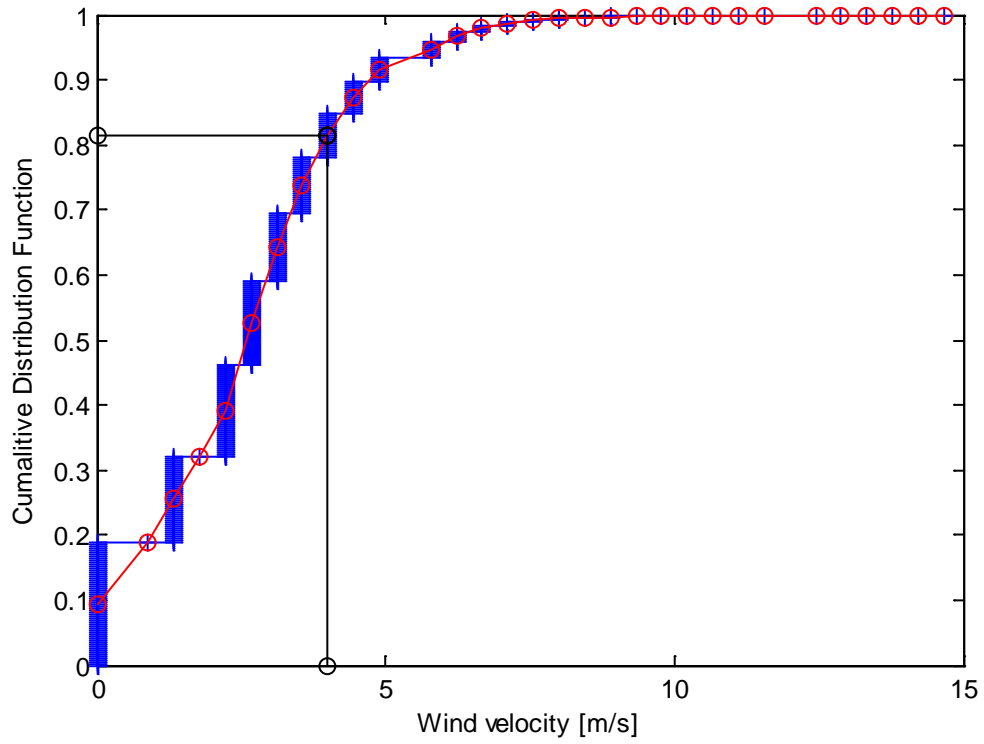


Figure 8. CDF plot of wind velocity.

The next step in the statistical analysis was to determine what the power output of the turbine would be in the Monterey Airport wind conditions. The power curve of the 4 kW vertical-axis wind turbine, which was provided by Urban Green Energy, is shown in Figure 9.

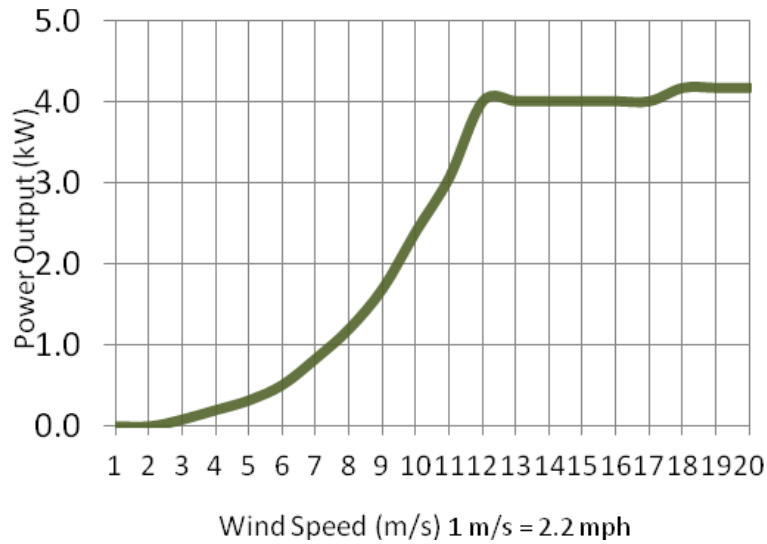


Figure 9. Power output vs. wind speed. From [19].

The data from Figure 9 was interpolated with the wind speed data from Monterey Airport in order to determine the power output of a single wind turbine at the NPS Turbopropulsion Laboratory. The results are shown in Figure 10, which shows that peak power is limited to just over 4 kW.

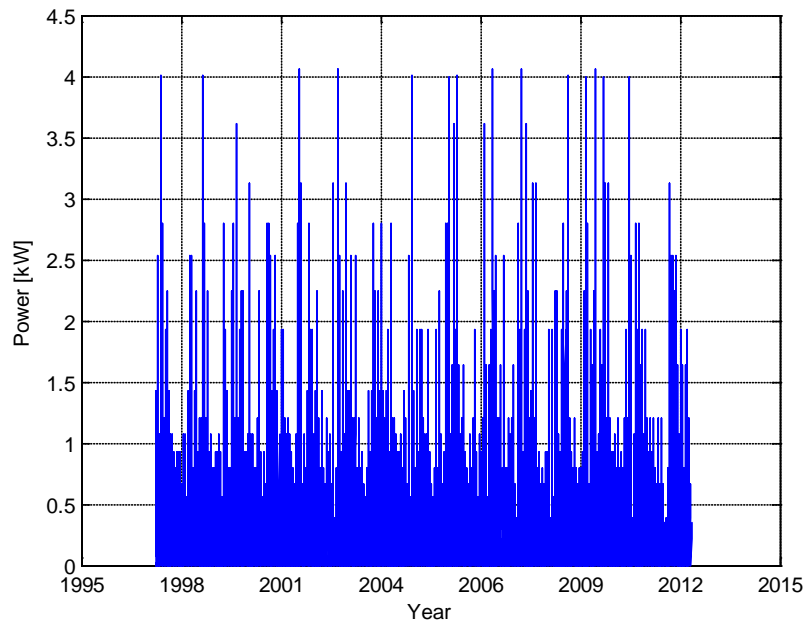


Figure 10. Power vs. time.

Energy is defined as the amount of power used over time. The direct relationship between energy (E) and power (P) is shown in Equation 1.

$$E = \int P dt \quad (1)$$

In order to determine the amount of energy captured annually from a single turbine, cumulative trapezoidal integration was used. In this method, the cumulative integral of power was calculated with respect to time using trapezoidal integration. The total energy captured by the 4 kW turbine would have been 18,748 kW-hours. Dividing this value by the total number of years of data yields 1,277.4 kW-hours per year. This value is the energy captured annually by one turbine. Since two turbines will be used at the NPS demonstration plant, the total energy captured will be 2,554.8 kW-hours annually.

III. PLANT ARCHITECTURE

The ultimate goal of this project was to develop a working demonstration plant of a thermal storage unit in a renewable powered cooling system. A typical cooling system uses a large battery for energy storage, rather than thermal energy. An example of this type of schematic is shown in Figure 11.

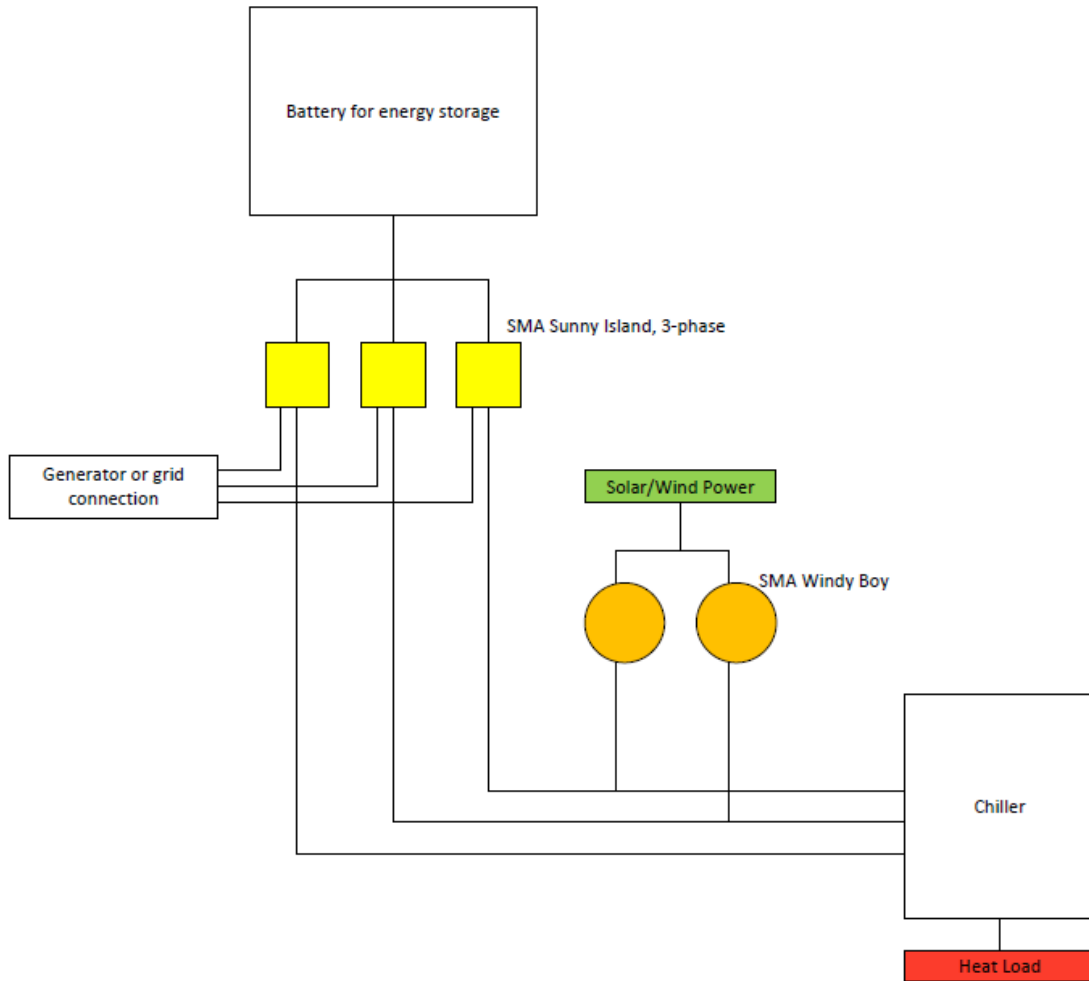


Figure 11. Typical cooling schematic.

The proposed demonstration plant will operate according to the schematic shown in Figure 12.

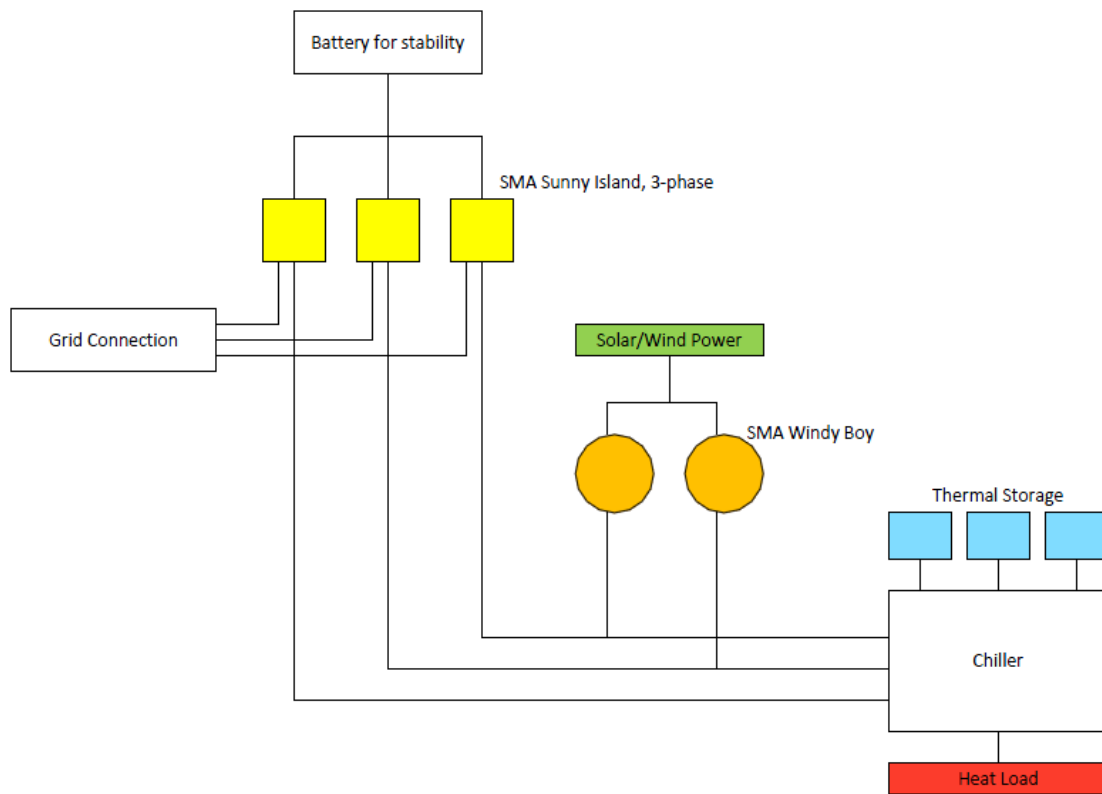


Figure 12. Proposed demonstration plant schematic.

The demonstration plant will be set-up at the NPS Turbopropulsion Laboratory. An overhead Google Maps view of the lab is shown in Figure 13.

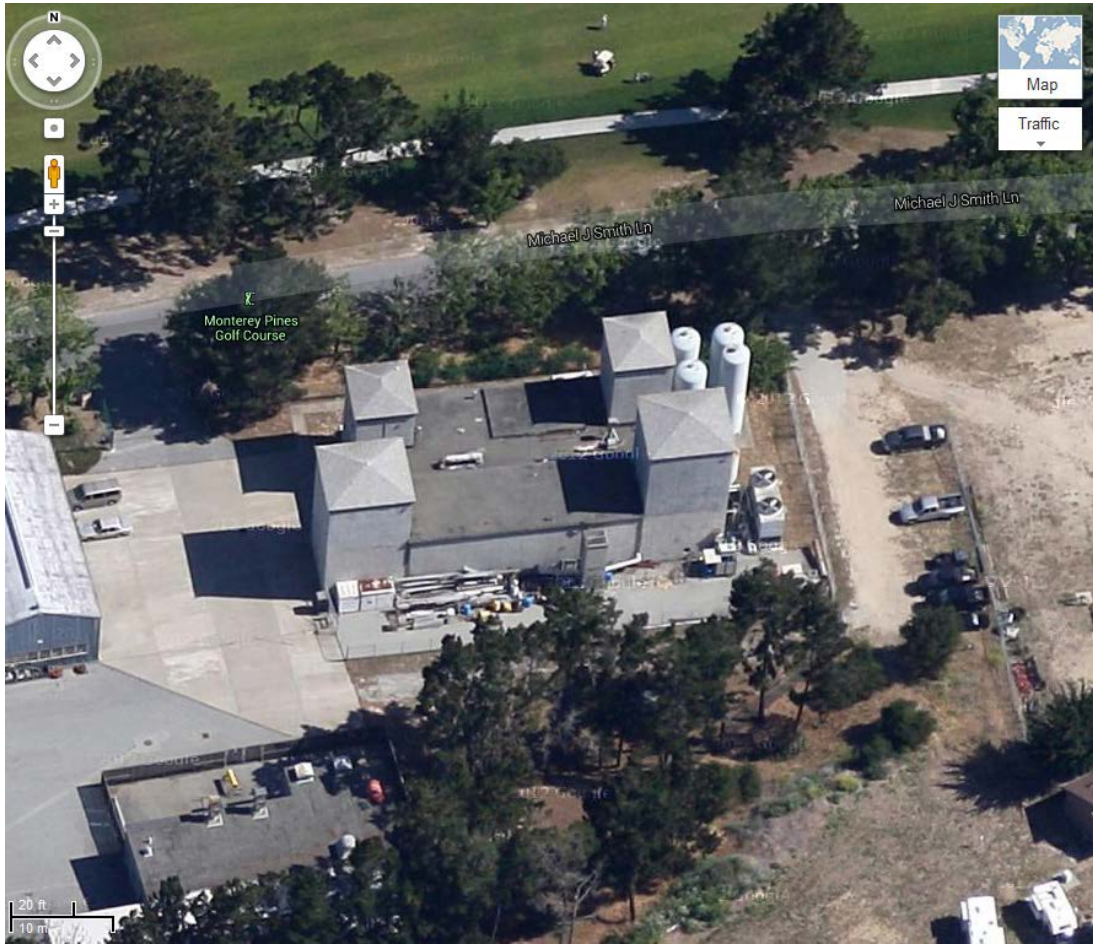


Figure 13. Google Maps image of NPS Turbopropulsion Laboratory.

The SolidWorks schematic of the lab, with a to-scale version of the electrical system, chiller, and thermal storage tanks, is shown in Figure 14. The individual components of the system will be discussed below.

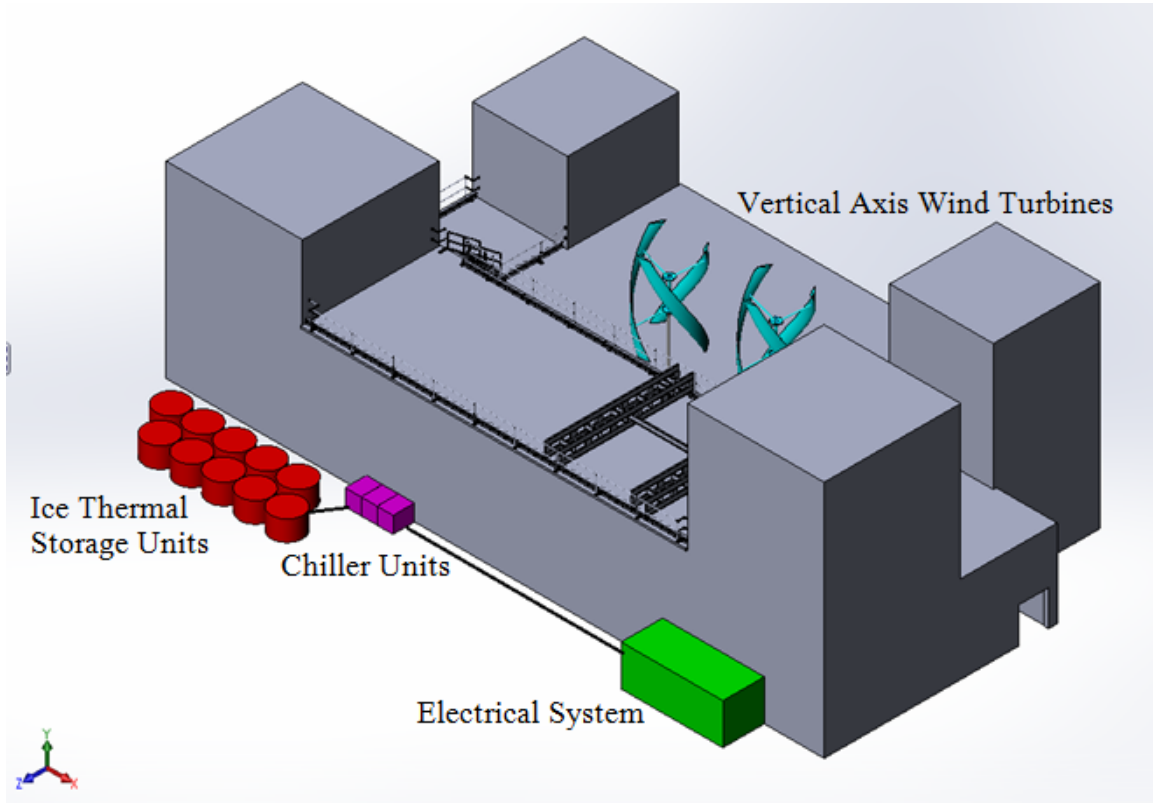


Figure 14. SolidWorks model of NPS Turbopropulsion Laboratory, including electrical system, chiller, and thermal storage tanks.

A. WIND TURBINE AND WINDY BOY INVERTERS

Wind turbines use the wind's energy to produce electricity. When wind moves over a turbine's blades, it creates a pressure differential. This pressure differential causes the blades to turn around a rotor, which is attached to a low-speed shaft. The low-speed shaft is connected to a high-speed shaft by a gear box, which increases the rotational speed. The high-speed shaft drives the generator, which produces alternating current (AC) electricity. The turbine is connected to a wind-interface box, which rectifies the current, converting "wild" AC to direct current (DC). The wind-interface box is then connected to a wind inverter, which converts the DC back into useable 50/60 Hz AC.

In this demonstration plant, two 4-kW vertical axis wind turbines will be used to power the system. The turbines, from Urban Green Energy, are shown in Figure 15.



Figure 15. Urban Green Energy 4 kW Vertical Axis Turbine. From [19].

These turbines will each be connected to an SMA Windy Boy inverter, which will yield the usable AC

B. CHILLER SYSTEM AND THERMAL ENERGY STORAGE

In this demonstration plant, the chiller is powered by the wind turbines to produce cooling. This system will implement Trane's Air-Cooled Liquid Chiller Model CGAM. This chiller is variable-speed, meaning that its speed will be set to match the amount of wind power entering the system. Large variable-speed chillers are common, but smaller units are not yet widely available. This chiller has a 26.4 kW (7.5 ton) capacity and will be placed outdoors.

The chiller will be connected to thermal ice storage tanks. When the wind turbines are spinning, the derived power will be used to operate the chiller. However, when wind output is low, the ice in the storage tank will melt. The high energy that can be absorbed by

melting will then be used for cooling instead of for running the chiller. CALMAC Thermal Energy Storage tanks 1045A, shown in Figure 16, will be used in this system.



Figure 16. CALMAC Thermal Energy Storage tanks 1045A. From [20].

Each tank has a thermal storage capacity of 144 kWh (41 ton-hr), a volume of ice/water of 1550 liters (410 gallons), and a volume of coolant solution in the heat exchanger of 151 liters (40 gallons) [20]. The tank contains a spiral-wound, polypropylene-tube heat exchanger surrounded by water, shown in Figure 17.

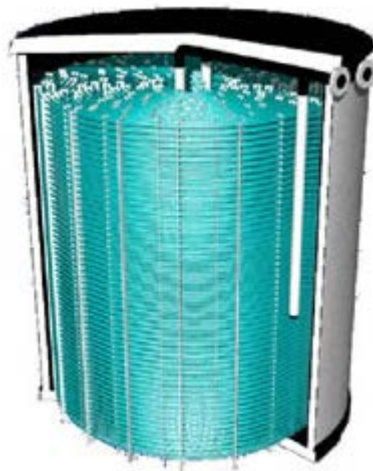


Figure 17. Inside of a CALMAC Thermal Energy Storage tank 1045A, with polypropylene tubing. From [20].

C. STABILITY BATTERY, GRID-CONNECTION, AND SMA SUNNY ISLAND

In a typical system, batteries are used as the primary means of storage, as shown in Figure 11. In this demonstration plant, the battery is required mainly for transient stability. Battery use is only required for 30 minutes at 25% power for lubrication immediately after startup. As previously discussed, batteries are costly and potentially dangerous. They would be eliminated for an ideal system on a forward-operating base.

Capacitors can be used if the battery system can be designed small enough. Capacitors charge and discharge much faster than batteries and are stored without charge, making them ideal for transport. Plus, a capacitor can be cycled many more times than a typical battery.

The demonstration plant will also be connected to the grid. This is not always feasible on forward-operating bases, where a generator would replace grid-connection.

The chiller that will be used in the demonstration plant is a 3-phase unit. Each of the wind turbine/SMA Windy Boy units will be connected to two of the three phase legs. The SMA Sunny Island inverters will automatically balance the load.

THIS PAGE INTENTIONALLY LEFT BLANK

IV. SOLIDIFICATION MODELING

A. INTRODUCTION

In a typical thermal storage tank, a coolant solution of 25% ethylene glycol and 75% water is cooled and circulated through a heat exchanger. In order to simplify the analysis, pure ethylene glycol was used in the simulation. The coolant, at a temperature of -5.56°C (22°F), extracts heat from the water until the water freezes. This process occurs until around 95% of the water has frozen. In order to gain a more detailed understanding of this process, an analysis of this procedure was completed using ANSYS Fluent. The goal of this analysis was to determine how the ice and tube thickness affected the solidification process. A secondary goal was to use the heat transfer rate and the solidification rate of ice to determine the volume of ice that formed around the tube.

The original goal of this analysis was to complete a transient analysis of the solidification of ice around the tube. Unfortunately, this analysis proved very difficult to complete, and a steady-state approach had to be used.

B. MODELING THE SYSTEM

The process began by modeling the tube in Design Modeler. A quarter section of the tube was modeled in order to simplify the simulation and minimize run times. CALMAC storage tanks are being used in this design project. The company provided the dimensions of the tube [20], which have a thickness of 0.0002 m, diameter of 0.02m, and length of 0.2 m. The tube was then surrounded by a layer of ice with a pre-determined thickness. The Design Modeler sketches are shown in Figure 18 and Figure 19.

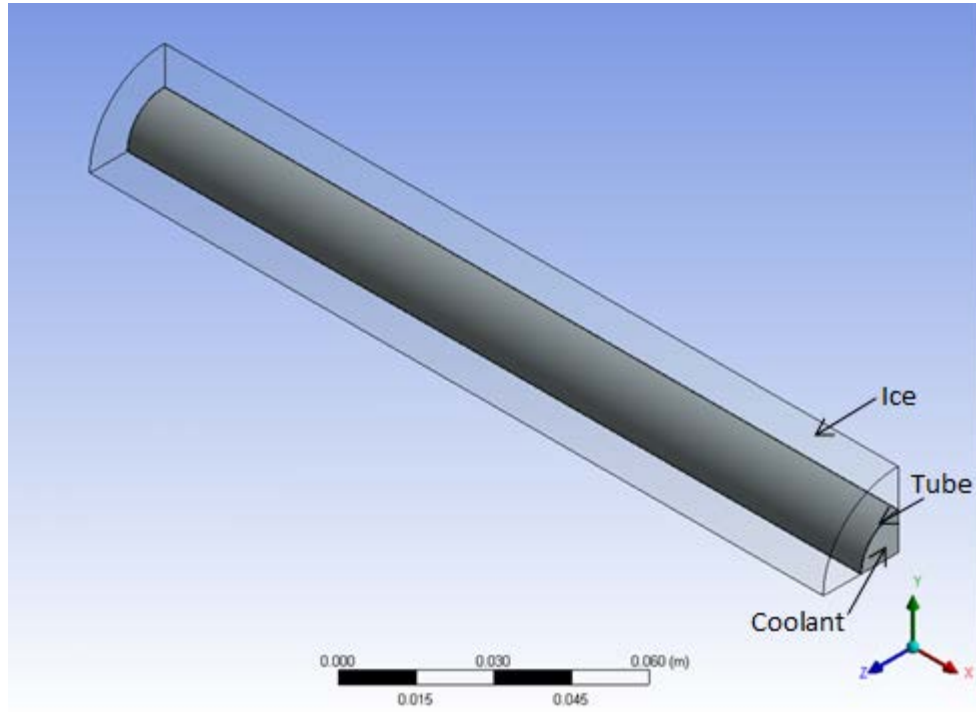


Figure 18. Quartered section of thermal ice storage system tubing.

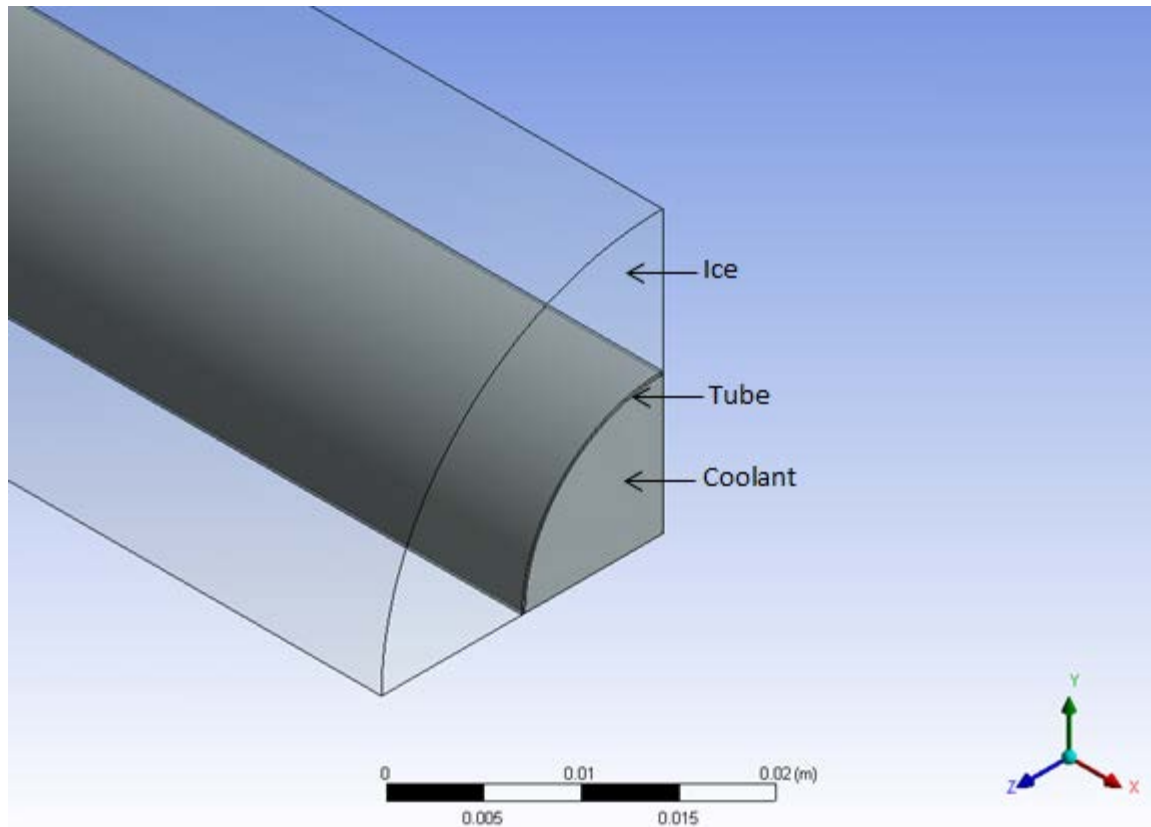


Figure 19. Quartered section of thermal ice storage system tubing—Detail.

Once the sketch was complete in Design Modeler, it was uploaded into ANSYS Workbench. Each component of the sketch, which included the inner tube which contained the ethylene-glycol solution, the tube itself, and the outer ice layer, was meshed separately. Figure 20 shows the mesh of the tube, with a thickness of 0.0002 m and an ice layer with thickness of 0.0202 m.

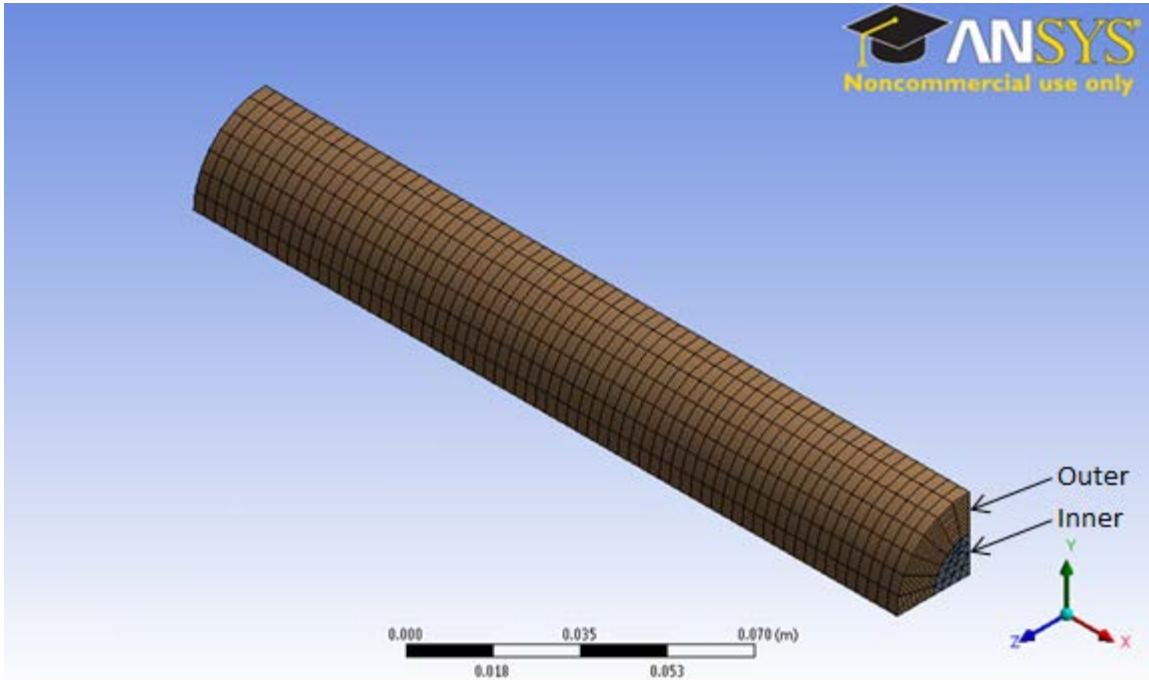


Figure 20. Mesh of quartered tube section.

The Sweep Method was used in the meshing of the ice layer in order to account for the curvature of the tube, and the Inflation tool was used for the mesh of the inner tube, as shown clearly in Figure 21.

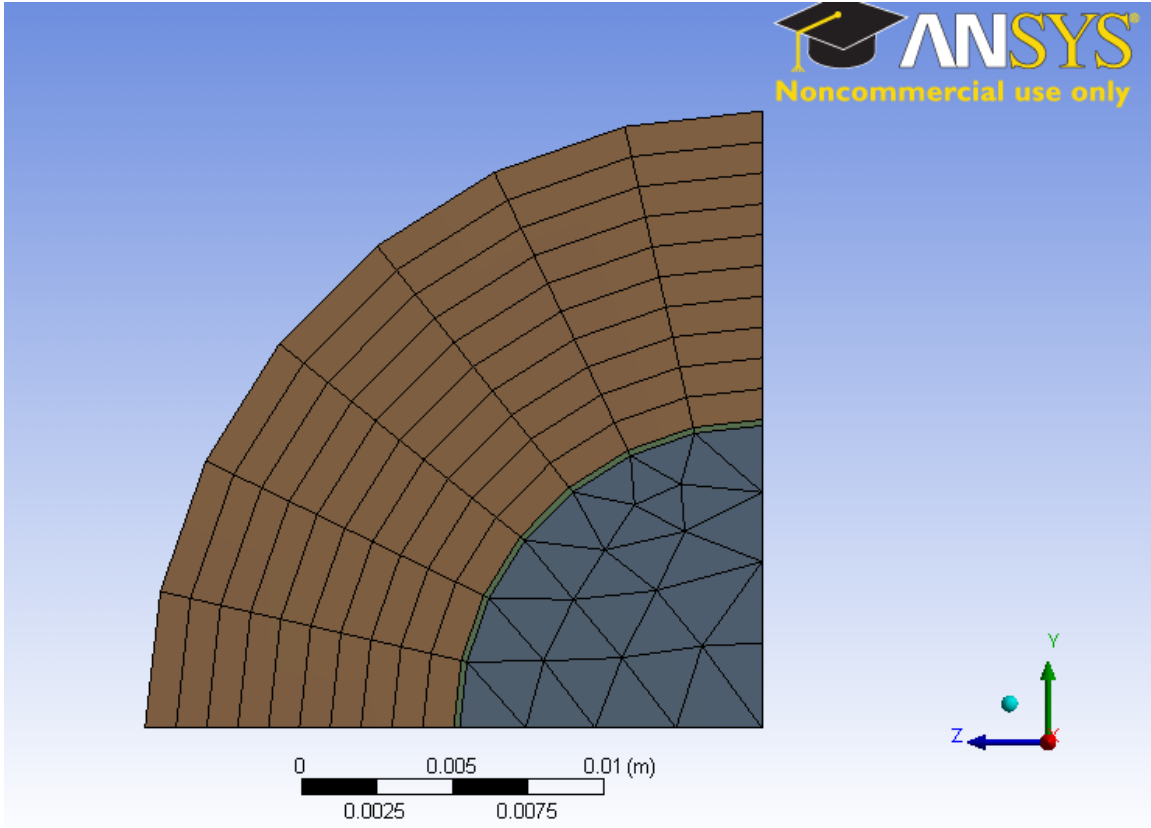


Figure 21. Sweep and inflation methods of meshing.

A numerical axisymmetric analysis was subsequently completed in ANSYS Fluent. The Energy, Radiation (Discrete Ordinates), and Viscous (Realizable k-epsilon, Enhanced Wall function) models were all turned on for the analysis. The inner tube material was designated as ethylene-glycol with an inner-inlet temperature of -5.65°C (21.83°F). The tube was designated as polypropylene. The outer layer was designated as ice with an inlet temperature of 0.00°C (32.00°F). Turbulent flow ethylene glycol was set to move through the tube at 4.4 m/s. This speed was derived using the formula for Reynolds number. Reynolds number (Re) for pipe flow is defined according to Equation 2.

$$\text{Re} = \frac{\rho v D}{\mu} \quad (2)$$

In Equation 2, ρ is density, v is average velocity, D is diameter, and μ is dynamic viscosity. For turbulent pipe flow, Reynolds number must be greater than 4000.

Knowing this and the values of ρ , D_H , and μ is density, v is velocity, D is diameter, and μ , it was possible to solve for velocity.

$$4000 = \frac{1111.4 \frac{kg}{m^3} \times v \times 0.02m}{0.0157 \frac{N \cdot s}{m^2}}$$

Solving for v yields a velocity of 2.83 m/s. In order to guarantee that the velocity would produce turbulent flow, the velocity for the simulations was increased to 4.4 m/s. This generated a Reynolds number of 6230, well into the turbulent regime.

Six runs using this method were completed, each using a different ice thickness surrounding the tube. The entire process was then repeated using a thinner wall tube with a thickness of 0.0004 m in order to determine the effect of wall thickness on ice growth. Appendix B shows an example of the temperature differentials throughout the tube during an example trial.

C. RESULTS

The FLUENT output report is shown in Appendix C. After each run was completed, the mass-weighted average enthalpy (J/kg) was recorded at the inlet and the outlet of the tube. The difference between these two values was taken and nondimensionalized to account for the length of the tube and the fact that the model was a quarter section. These values are shown in Appendix D, and the results are shown in Figure 22.

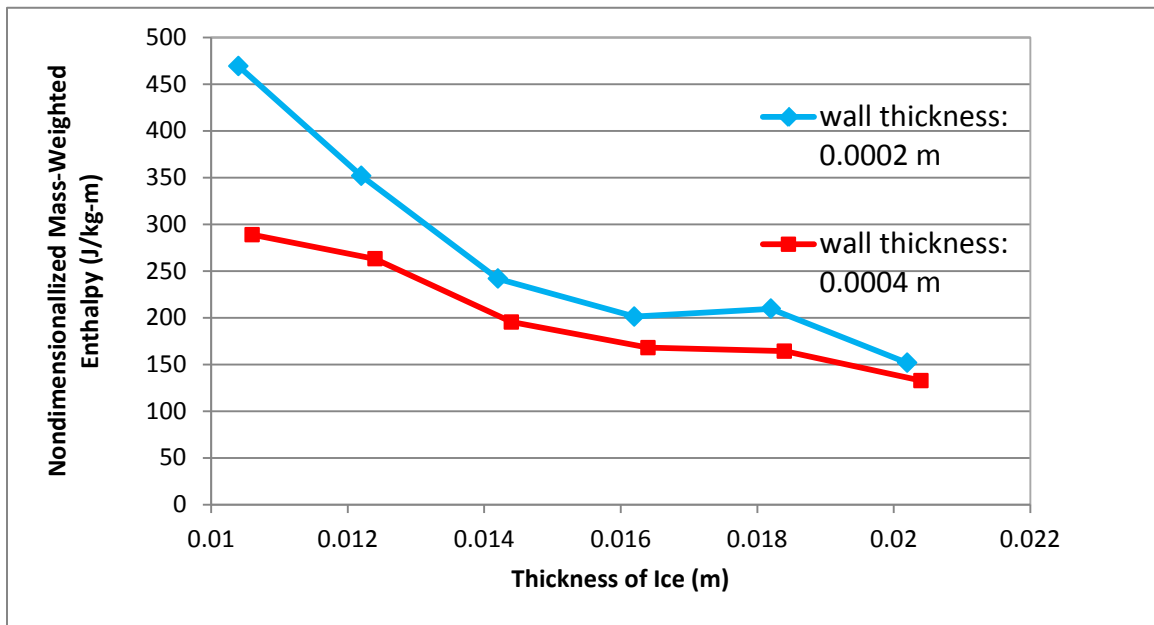


Figure 22. Nondimensionalized mass-weighted enthalpy vs. ice thickness.

The results show that as the thickness of the ice increases, the enthalpy difference between the inlet and outlet of the tube decreased. The slight upturn in data at an ice thickness of 0.018 m could likely be resolved by increasing the resolution of the mesh.

The total heat transfer rate (W) was also recorded for the inlet and outlet of the tube after each run. The difference between these two values was taken and nondimensionalized in the same manner as the mass-weighted average enthalpy. This value was divided by 1 second in order to determine an energy value, and then divided by the solidification rate, or the heat of fusion, of ice (334 kJ/kg) in order to determine the

mass of ice produced. Finally, the volume of ice was determined by dividing this value by the density of ice (916.2 kg/m^3). The results are shown in Figure 23.

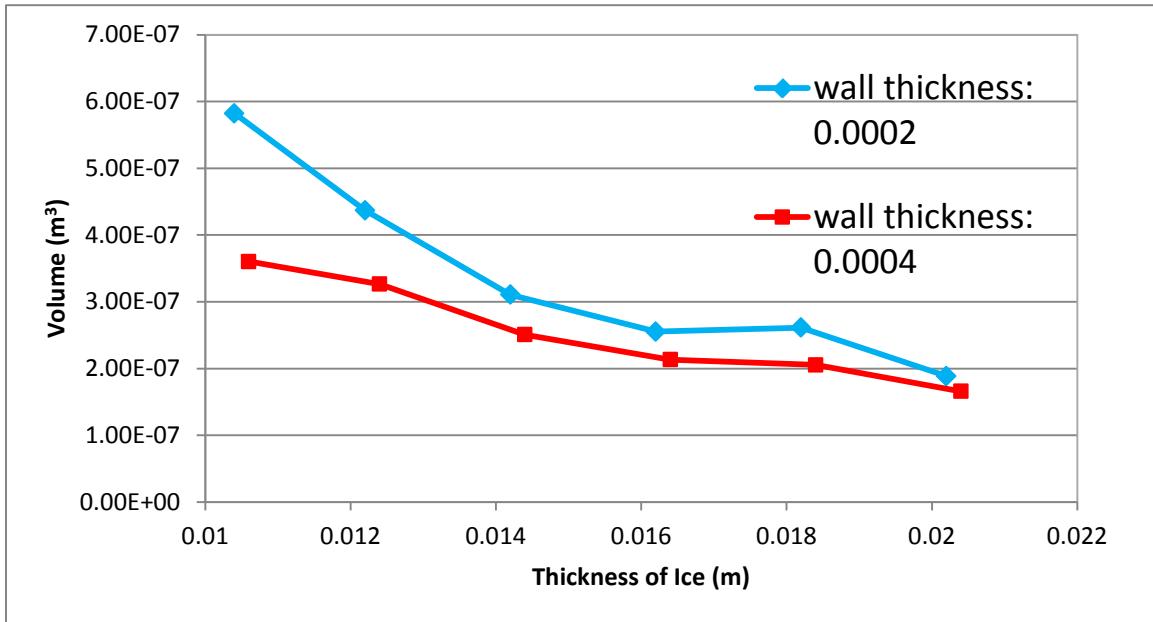


Figure 23. Volume of ice produced vs. thickness of ice.

The results show that as the thickness of the ice surrounding the tube increased, the volume of the ice that is produced decreases. The numerical results are shown in Appendix E.

Wall thickness affects the results: a thinner wall resulted in a greater enthalpy difference between the inlet and outlet therefore a greater volume of ice production. The space between tubes in the heat exchanger was estimated to be slightly greater than 0.02 m, or slightly larger than the diameter of the tube. When the thickness of the ice approached the tube separation distance, ice growth was smaller. However, it should be noted that in this simulation only one tube was modeled, so tube separation was not a limiting factor. The main conclusion that could be drawn was that the most important factor for ice enthalpy and volume change in this simulation was the thickness of the ice around the tube.

V. CONCLUSION

This thesis was integral for the development of the renewable energy demonstration plant at the NPS Turbopropulsion Laboratory. Developing renewable energy technology is important to both the United States government and military. The work done in this thesis is in accordance with the goals of both of these groups as they move toward energy independence. Projects like this will be especially useful in the transition to “net-zero” installations. A scaled-down version of this system can be especially valuable on forward-operating bases, while a scaled-up version will be useful for cooling data centers.

The analysis of the weather statistics was useful in choosing an appropriate turbine and determining the total power output of the turbine. 1,277.4 kW-hours of energy will be captured by one turbine per year. Two turbines will be used, meaning 2,554.8 kW-hours will be captured annually.

A separate analysis of ice solidification within the thermal ice storage system was also completed. These two analyses contributed to a more in-depth understanding of both the chiller and thermal ice storage system mechanisms. Ultimately it was found that the thickness of the ice had the most significant impact on the change in enthalpy through the tube and the amount of ice formed around the tube.

The various components of the renewable energy plant and their complex integration into the system were thoroughly explained. The system successfully incorporates wind turbines, an electrical system, chiller units, thermal ice storage units, a stability battery, and grid storage.

THIS PAGE INTENTIONALLY LEFT BLANK

VI. RECOMMENDATIONS

The next step going forward is to actually set up the demonstration plant and ensure that the various components can operate together. Once that is completed, the architecture of the demonstration plant can be improved. An extensive study of the various components will allow for the optimization of the system. This will predicate the use of the system in an alternative setting, such as a forward-operating base. Specifically, a study of what size wind turbine, what size chiller unit, and how many thermal storage tanks to use would be advantageous. In addition, making the system truly grid- and battery-independent can be an area of study.

A final important step is the implementation of solar panels into the system. Solar panels are another source of intermittent, renewable energy that can be used in parallel with the wind turbines to power the system. An analysis of solar conditions, similar to the wind analysis completed in this thesis, would be beneficial.

THIS PAGE INTENTIONALLY LEFT BLANK

APPENDIX A

```
% Matlab script file to read in wind data from Monterey Airport

clear all
close all

% Constant
Data.CutInSpeed = 4.0; % [m/s]

% Data is read in from file
[NUM,~,~]=xlsread('MRY_hourly_observations_1998-2012.xlsx');

% Date Data is separated
Data.String = num2str(NUM(:,2)); % Converts to
string
Data.Year = str2num(Data.String(:,1:4)); % Strips out years
Data.Month = str2num(Data.String(:,5:6)); % Strips out months
Data.Day = str2num(Data.String(:,7:8)); % Strips out days
Data.Hour = str2num(Data.String(:,9:10)); % Strips out hours

% Windspeed Data is separated
Data.Wind = NUM(:,4); % Wind Velocity in
mph
Data.Wind = 1.6*Data.Wind/3.6; % Wind Velocity in
m/s
Data.WindCDF = sort(Data.Wind(~isnan(Data.Wind))); % Not-a-Numbers
(nans excluded)

% To eliminate NaN
Data.Wind(isnan(Data.Wind)) = 0;

% CDF data (p is stats examples)
Data.p = linspace(0,1,size(Data.WindCDF,1));
[x(:,1),IA,IC] = unique(Data.WindCDF); % Keep only 1 data
at each speed
y(:,1) = (Data.p(IA))';
[x(:,2),IA,IC] = unique(Data.WindCDF,'first'); % Keep only 1 data
at each speed
y(:,2) = (Data.p(IA))';

% average of the two
x = mean(x,2);
y = mean(y,2);

% Cut in speed probability is found
Data.CutInSpeedCDF = interp1(x,y,Data.CutInSpeed); % Probability
disp('Cut in speed CDF') Data.CutInSpeedCDF

% Date is converted to Matlab date numbering system Data.DateNumber =
datenum(Data.Year,Data.Month,Data.Day,Data.Hour,zeros(size(Data.Hour)),
zeros(size(Data.Hour)));
```

```

% Windspeed is plotted against dates
figure(1); close; figure(1);
plot(Data.DateNumber,Data.Wind); grid on
datetick('x',10,'kepticks','keeplimits');
ylabel('Windvelocity [m/s]'); xlabel('Year')

% Plot integral of windspeed distribution figure(2); close; figure(2);
plot(Data.WindCDF,Data.p,'+-b'); hold on
plot(x,y,'-or')
plot(Data.CutInSpeed,Data.CutInSpeedCDF,'ok')
plot([Data.CutInSpeed Data.CutInSpeed],[0 Data.CutInSpeedCDF],'-ok')
plot([0 Data.CutInSpeed],[Data.CutInSpeedCDF Data.CutInSpeedCDF],'-ok')
ylabel('Cumalitive Distribution Function'); xlabel('Windvelocity
[m/s]')

% Data fitting
%figure(3); close; figure(3);
%plot(Data.WindCDF,log(-log(1-Data.p)));
clear Data.String NUM % Memory cleanup

[NUM,~,~]=xlsread('Turbine_Specifications.xlsx')

WindTurb.WindVel=NUM(:,1);
WindTurb.Power=NUM(:,2);

P=interp1(WindTurb.WindVel,WindTurb.Power,Data.Wind);

%plot of power vs. time
figure(3);close;figure(3);
plot(Data.DateNumber,P);grid on;
datetick('x',10,'kepticks','keeplimits');
ylabel('Power [kW]'); xlabel('Year')

%plot of energy vs. time

E.total=cumtrapz(Data.DateNumber*24,P);

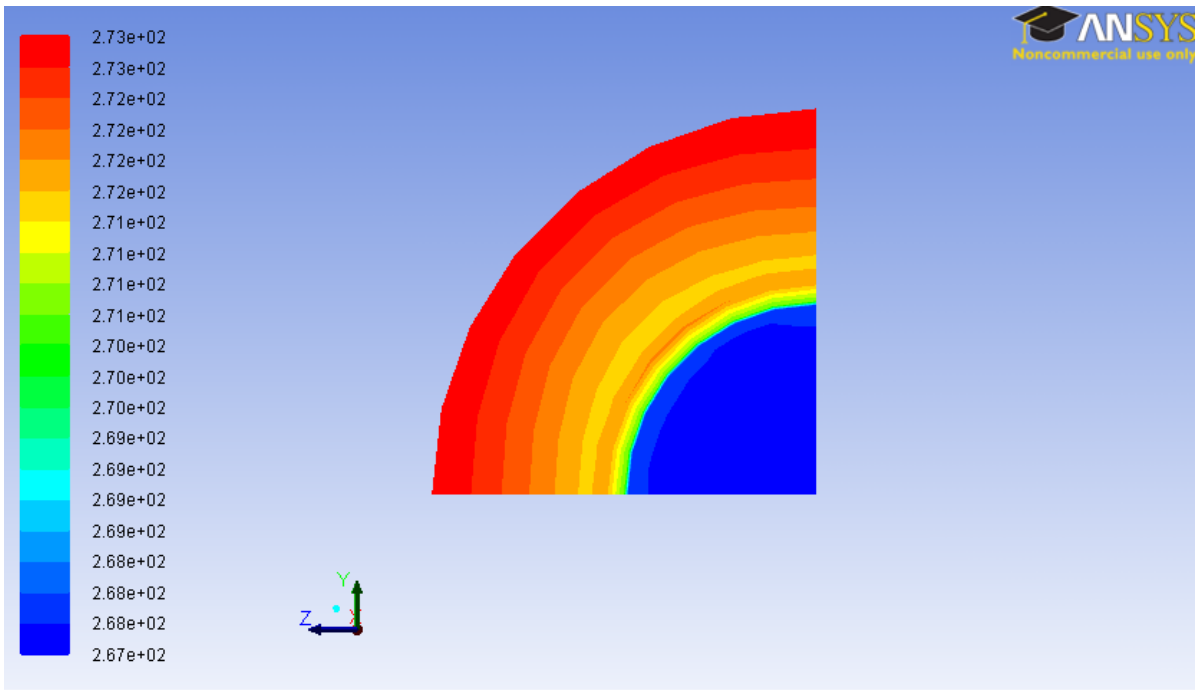
figure(4);close;figure(4);
plot(Data.DateNumber,E.total);grid on;
ylabel('Energy [kW-hour]'); xlabel('Year'); datetick('x');

Data.years=(Data.DateNumber(end)-Data.DateNumber(1))/365;

E.annual=E.total(end)/Data.years

```

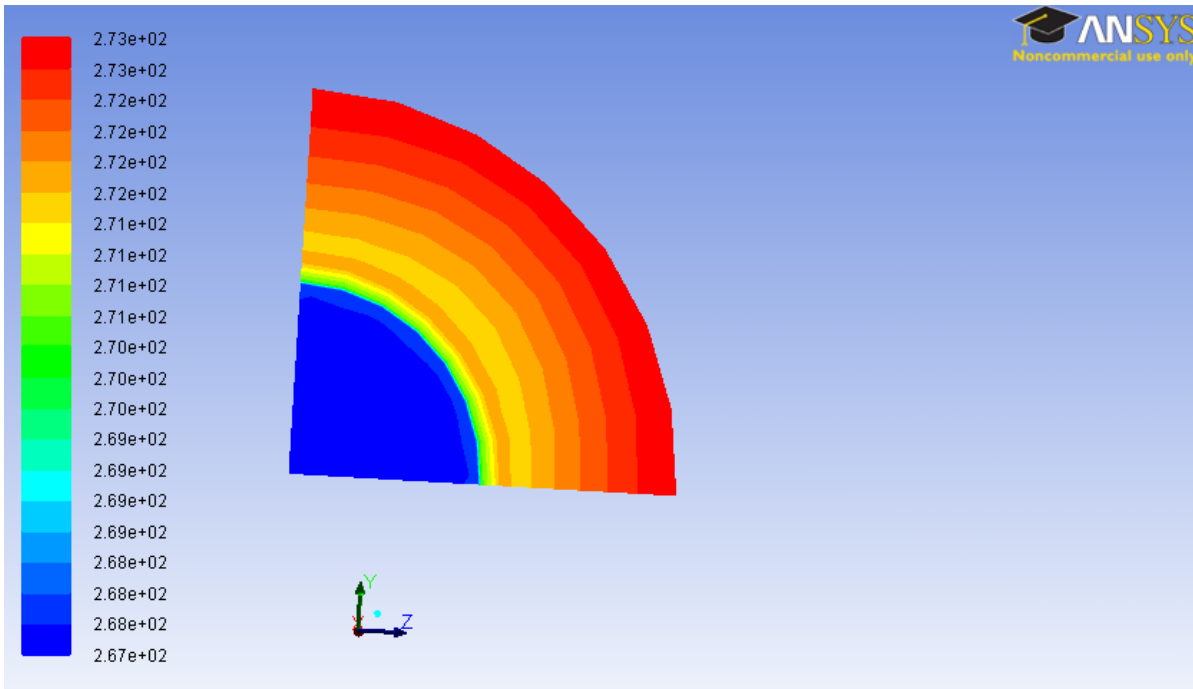
APPENDIX B



Contours of Static Temperature (k)

May 07, 2013
ANSYS FLUENT 14.0 (3d, dp, pbns, rke)

Figure 24. Inlet with a tube thickness of 0.0002 m and an ice thickness of 0.0204 m



Contours of Static Temperature (k)

May 07, 2013
ANSYS FLUENT 14.0 (3d, dp, pbns, rke)

Figure 25. Outlet with a tube thickness of 0.0002 m and an ice thickness of 0.0204 m

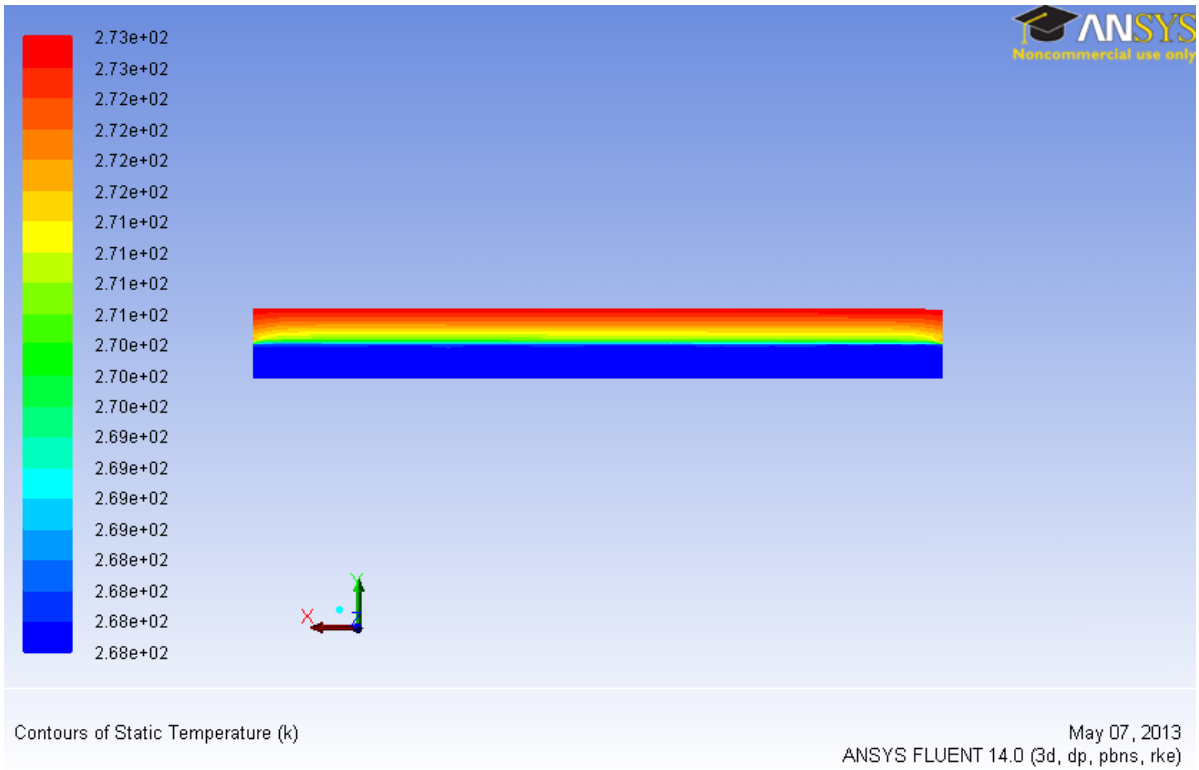


Figure 26. Side view of a tube with thickness of 0.0002 m and an ice thickness of 0.0204 m

THIS PAGE INTENTIONALLY LEFT BLANK

APPENDIX C

report

FLUENT
 Version: 3d, dp, pbns, rke (3d, double precision, pressure-based, realizable
 k-epsilon)
 Release: 14.0.0
 Title:

Models

Model	Settings
Space	3D
Time	Steady
Viscous	Realizable k-epsilon turbulence model
Wall Treatment	Enhanced Wall Treatment
Heat Transfer	Enabled
Solidification and Melting	Disabled
Radiation	Discrete Ordinate Model
Species	Disabled
Coupled Dispersed Phase	Disabled
NOx Pollutants	Disabled
SOx Pollutants	Disabled
Soot	Disabled
Mercury Pollutants	Disabled

Material Properties

Material: ice_1 (solid)

Property	Units	Method	Value(s)
Density	kg/m3	constant	916.20001
Cp (Specific Heat)	j/kg-k	constant	2050
Thermal Conductivity	w/m-k	constant	2.22
Absorption Coefficient	1/m	constant	0
Scattering Coefficient	1/m	constant	0
Scattering Phase Function		isotropic	#f
Refractive Index		constant	1

Material: polypropylene (solid)

Property	Units	Method	Value(s)
Density	kg/m3	constant	946
Cp (Specific Heat)	j/kg-k	constant	1800
Thermal Conductivity	w/m-k	constant	0.15000001
Absorption Coefficient	1/m	constant	0
Scattering Coefficient	1/m	constant	0
Scattering Phase Function		isotropic	#f
Refractive Index		constant	1

Material: ethylene-glycol (fluid)

Property	Units	Method	Value(s)
Density	kg/m3	constant	1111.4
Cp (Specific Heat)	j/kg-k	constant	2415
Thermal Conductivity	w/m-k	constant	0.252
Viscosity	kg/m-s	constant	0.0157
Molecular Weight	kg/kgmol	constant	62.0482
Absorption Coefficient	1/m	constant	0

Page 1

Scattering Coefficient	report 1/m	constant	0
Scattering Phase Function		isotropic	#f
Thermal Expansion Coefficient	1/k	constant	0
Refractive Index		constant	1
Speed of Sound	m/s	none	#f

Material: ice (fluid)

Property	Units	Method	value(s)

Density	kg/m3	constant	915
Cp (Specific Heat)	j/kg-k	polynomial	(200-273.15:
-18.123364 7.809018 0 0 0) (273.15-273.15: 0 0 0 0 0)			0 0)
Thermal Conductivity	w/m-k	constant	0.0454
Viscosity	kg/m-s	constant	1.72e-05
Molecular Weight	kg/kgmol	constant	18.01534
Absorption Coefficient	1/m	constant	0
Scattering Coefficient	1/m	constant	0
Scattering Phase Function		isotropic	#f
Thermal Expansion Coefficient	1/k	constant	0
Refractive Index		constant	1
Speed of Sound	m/s	none	#f

Material: aluminum (solid)

Property	Units	Method	value(s)

Density	kg/m3	constant	2719
Cp (Specific Heat)	j/kg-k	constant	871
Thermal Conductivity	w/m-k	constant	202.4
Absorption Coefficient	1/m	constant	0
Scattering Coefficient	1/m	constant	0
Scattering Phase Function		isotropic	#f
Refractive Index		constant	1

Cell Zone Conditions

Zones

name	id	type
part-outer_fluid	8	solid
part-pipe	9	solid
part-inner_fluid	7	fluid

Setup Conditions

part-outer_fluid

Condition	report	value
Material Name		ice_1
Specify source terms?		no
Source Terms		((energy))
Specify fixed values?		no
Fixed Values		((temperature (inactive
. #f) (constant . 0) (profile))		
Frame Motion?		no
Relative To Cell Zone		-1
Reference Frame Rotation Speed (rad/s)		0
Reference Frame X-Velocity Of Zone (m/s)		0
Reference Frame Y-Velocity Of Zone (m/s)		0
Reference Frame Z-Velocity Of Zone (m/s)		0
Reference Frame X-Origin of Rotation-Axis (m)		0
Reference Frame Y-Origin of Rotation-Axis (m)		0
Reference Frame Z-Origin of Rotation-Axis (m)		0
Reference Frame X-Component of Rotation-Axis		0
Reference Frame Y-Component of Rotation-Axis		0
Reference Frame Z-Component of Rotation-Axis		1
Reference Frame User Defined Zone Motion Function		none
Mesh Motion?		no
Relative To Cell Zone		-1
Moving Mesh Rotation Speed (rad/s)		0
Moving Mesh X-velocity Of Zone (m/s)		0
Moving Mesh Y-Velocity Of Zone (m/s)		0
Moving Mesh Z-Velocity Of Zone (m/s)		0
Moving Mesh X-Origin of Rotation-Axis (m)		0
Moving Mesh Y-Origin of Rotation-Axis (m)		0
Moving Mesh Z-Origin of Rotation-Axis (m)		0
Moving Mesh X-Component of Rotation-Axis		0
Moving Mesh Y-Component of Rotation-Axis		0

	report	
Moving Mesh Z-Component of Rotation-Axis		1
Moving Mesh User Defined Zone Motion Function		none
Participates in radiation		yes
Deactivated Thread		no
part-pipe		
Condition		value

Material Name		polypropylene
Specify source terms?		no
Source Terms		((energy))
Specify fixed values?		no
Fixed Values		((temperature (inactive
. #f) (constant . 0) (profile)))		
Frame Motion?		no
Relative To Cell Zone		-1
Reference Frame Rotation Speed (rad/s)		0
Reference Frame X-Velocity Of Zone (m/s)		0
Reference Frame Y-Velocity Of Zone (m/s)		0
Reference Frame Z-Velocity Of Zone (m/s)		0
Reference Frame X-Origin of Rotation-Axis (m)		0
Reference Frame Y-Origin of Rotation-Axis (m)		0
Reference Frame Z-Origin of Rotation-Axis (m)		0
Reference Frame X-Component of Rotation-Axis		0
Reference Frame Y-Component of Rotation-Axis		0
Reference Frame Z-Component of Rotation-Axis		1
Reference Frame User Defined Zone Motion Function		none
Mesh Motion?		no
Relative To Cell Zone		-1
Moving Mesh Rotation Speed (rad/s)		0
Moving Mesh X-Velocity Of Zone (m/s)		0
Moving Mesh Y-Velocity Of Zone (m/s)		0
Moving Mesh Z-Velocity Of Zone (m/s)		0

report

Moving Mesh X-Origin of Rotation-Axis (m)	0
Moving Mesh Y-Origin of Rotation-Axis (m)	0
Moving Mesh Z-Origin of Rotation-Axis (m)	0
Moving Mesh X-Component of Rotation-Axis	0
Moving Mesh Y-Component of Rotation-Axis	0
Moving Mesh Z-Component of Rotation-Axis	1
Moving Mesh User Defined Zone Motion Function	none
Participates in radiation	no
Deactivated Thread	no

part-inner_fluid

Condition	Value
-----------	-------

Material Name	ethylene-glycol
---------------	-----------------

Specify source terms?	no
-----------------------	----

Source Terms (x-momentum) (y-momentum) (z-momentum) (k) (epsilon) (energy))	((mass)
--	---------

Specify fixed values?	no
-----------------------	----

Local coordinate system for Fixed velocities	no
--	----

Fixed Values (inactive . #f) (constant . 0) (profile)) (y-velocity (inactive . #f) (constant . 0) (profile)) (z-velocity (inactive . #f) (constant . 0) (profile)) (k (inactive . #f) (constant . 0) (profile)) (epsilon (inactive . #f) (constant . 0) (profile)) (temperature (inactive . #f) (constant . 0) (profile)))	((x-velocity
---	--------------

Frame Motion?	report	no
Relative To Cell Zone		-1
Reference Frame Rotation Speed (rad/s)		0
Reference Frame X-Velocity of Zone (m/s)		0
Reference Frame Y-Velocity of Zone (m/s)		0
Reference Frame Z-Velocity of Zone (m/s)		0
Reference Frame X-Origin of Rotation-Axis (m)		0
Reference Frame Y-Origin of Rotation-Axis (m)		0
Reference Frame Z-Origin of Rotation-Axis (m)		0
Reference Frame X-Component of Rotation-Axis		0
Reference Frame Y-Component of Rotation-Axis		0
Reference Frame Z-Component of Rotation-Axis		1
Reference Frame User Defined Zone Motion Function		none

report

Mesh Motion?	no
Relative To Cell Zone	-1
Moving Mesh Rotation Speed (rad/s)	0
Moving Mesh X-velocity Of Zone (m/s)	0
Moving Mesh Y-velocity Of Zone (m/s)	0
Moving Mesh Z-velocity Of Zone (m/s)	0
Moving Mesh X-Origin of Rotation-Axis (m)	0
Moving Mesh Y-Origin of Rotation-Axis (m)	0
Moving Mesh Z-Origin of Rotation-Axis (m)	0
Moving Mesh X-Component of Rotation-Axis	0
Moving Mesh Y-Component of Rotation-Axis	0
Moving Mesh Z-Component of Rotation-Axis	1
Moving Mesh User Defined Zone Motion Function	none

report

Participates in radiation	yes
Deactivated Thread	no
Laminar zone?	no
Set Turbulent Viscosity to zero within laminar zone?	yes
Embedded Subgrid-scale Model	0
Momentum Spatial Discretization	0
Cwale	0.325
Cs	0.1
Porous zone?	no
Conical porous zone?	no
X-Component of Direction-1 Vector	1
Y-Component of Direction-1 Vector	0

	report
Z-Component of Direction-1 Vector	0
X-Component of Direction-2 Vector	0
Y-Component of Direction-2 Vector	1
Z-Component of Direction-2 Vector	0
X-Component of Cone Axis Vector	1
Y-Component of Cone Axis Vector	0
Z-Component of Cone Axis Vector	0
X-Coordinate of Point on Cone Axis (m)	1
Y-Coordinate of Point on Cone Axis (m)	0
Z-Coordinate of Point on Cone Axis (m)	0
Half Angle of Cone Relative to its Axis (deg)	0
Relative Velocity Resistance Formulation?	yes
Direction-1 Viscous Resistance (1/m ²)	0

report

Direction-2 Viscous Resistance (1/m ²)	0
Direction-3 Viscous Resistance (1/m ²)	0
Choose alternative formulation for inertial resistance?	no
Direction-1 Inertial Resistance (1/m)	0
Direction-2 Inertial Resistance (1/m)	0
Direction-3 Inertial Resistance (1/m)	0
C0 Coefficient for Power-Law	0
C1 Coefficient for Power-Law	0
Porosity	1
Equilibrium Thermal Model (if no, Non-Equilibrium)?	yes
Non-Equilibrium Thermal Model?	no
Solid Material Name	aluminum

Interfacial Area Density (1/m)	report	1
Heat Transfer Coefficient (w/m2-k)		1

Boundary Conditions

Zones

name	id	type
outer_outlet	15	wall
outer_inlet	13	wall
wall-part-inner_fluid-part-pipe-shadow	23	wall
wall-part-pipe	1	wall
wall-part-inner_fluid-part-pipe	3	wall
inner_inlet	12	velocity-inlet
inner_outlet	14	pressure-outlet
symmetry_1-part-inner_fluid	17	symmetry
symmetry_1-part-pipe	19	symmetry
symmetry_1-part-outer_fluid	18	symmetry
symmetry_2-part-inner_fluid	20	symmetry
symmetry_2-part-pipe	22	symmetry
symmetry_2-part-outer_fluid	21	symmetry
wall	10046	wall

Setup Conditions

outer_outlet

Condition	value
Wall Thickness (m)	0
Heat Generation Rate (w/m3)	0
Material Name	ice_1
Thermal BC Type	1
Temperature (k)	300
Heat Flux (w/m2)	0
Convective Heat Transfer Coefficient (w/m2-k)	0
Free Stream Temperature (k)	300
Enable shell conduction?	no
Wall Motion	0
Shear Boundary Condition	0

```

report
Define wall motion relative to adjacent cell zone?      yes
Apply a rotational velocity to this wall?              no
Velocity Magnitude (m/s)                              0
X-Component of wall Translation                        1
Y-Component of wall Translation                        0
Z-Component of wall Translation                        0
Define wall velocity components?                      no
X-Component of wall Translation (m/s)                 0
Y-Component of wall Translation (m/s)                 0
Z-Component of wall Translation (m/s)                 0
Internal Emissivity                                   1
External Emissivity                                   1
External Radiation Temperature (k)                   300
Radiation BC Type                                     3
X-Component of Radiation Direction                   1
Y-Component of Radiation Direction                   0
Z-Component of Radiation Direction                   0
Theta Width of Beam (deg)
9.9923854e-07
Phi width of Beam (deg)
9.9923854e-07
(((constant . 0) (profile )))
(((constant . 0) (profile )))
(1)
Apply Direct Irradiation Parallel to the Beam?      no
Use Beam Direction from Solar Load Model Settings   no
Use Direct and Diffuse Irradiation from Solar Load Model Settings no
Rotation Speed (rad/s)                              0
X-Position of Rotation-Axis Origin (m)              0
Y-Position of Rotation-Axis Origin (m)              0
Z-Position of Rotation-Axis Origin (m)              0
X-Component of Rotation-Axis Direction              1
Y-Component of Rotation-Axis Direction              0

```

Z-Component of Rotation-Axis Direction	report	0
X-component of shear stress (pascal)		0
Y-component of shear stress (pascal)		0
Z-component of shear stress (pascal)		0
Fslip constant		0
Eslip constant		0
Surface tension gradient (n/m-k)		0
Specularity Coefficient		0

outer_inlet

Condition	value
-----------	-------

Wall Thickness (m)	0
Heat Generation Rate (w/m3)	0
Material Name	ice_1
Thermal BC Type	1
Temperature (k)	273
Heat Flux (w/m2)	0
Convective Heat Transfer Coefficient (w/m2-k)	0
Free Stream Temperature (k)	300
Enable shell conduction?	no
Wall Motion	0
Shear Boundary Condition	0
Define wall motion relative to adjacent cell zone?	yes
Apply a rotational velocity to this wall?	no
Velocity Magnitude (m/s)	0.001
X-Component of Wall Translation	1
Y-Component of Wall Translation	0
Z-Component of wall Translation	0
Define wall velocity components?	no
X-Component of Wall Translation (m/s)	0
Y-Component of Wall Translation (m/s)	0

```

report
Z-Component of Wall Translation (m/s) 0
Internal Emissivity 1
External Emissivity 1
External Radiation Temperature (k) 300
Radiation BC Type 3
X-Component of Radiation Direction 1
Y-Component of Radiation Direction 0
Z-Component of Radiation Direction 0
Theta Width of Beam (deg)
9.9923854e-07
Phi Width of Beam (deg)
9.9923854e-07
(((constant . 0) (profile )))
(((constant . 0) (profile ))) (1)
Apply Direct Irradiation Parallel to the Beam? no
Use Beam Direction from Solar Load Model Settings no
Use Direct and Diffuse Irradiation from Solar Load Model Settings no
Rotation Speed (rad/s) 0
X-Position of Rotation-Axis Origin (m) 0
Y-Position of Rotation-Axis Origin (m) 0
Z-Position of Rotation-Axis Origin (m) 0
X-Component of Rotation-Axis Direction 1
Y-Component of Rotation-Axis Direction 0
Z-Component of Rotation-Axis Direction 0
X-component of shear stress (pascal) 0
Y-component of shear stress (pascal) 0
Z-component of shear stress (pascal) 0
Fslip constant 0
Eslip constant 0
Surface tension gradient (n/m-k) 0
Specularity Coefficient 0

```

report

Condition	value

aluminum	
Wall Thickness (m)	0
Heat Generation Rate (w/m3)	0
Material Name	
Thermal BC Type	3
Temperature (k)	300
Heat Flux (w/m2)	0
Convective Heat Transfer Coefficient (w/m2-k)	0
Free Stream Temperature (k)	300
Enable shell conduction?	no
Wall Motion	0
Shear Boundary Condition	0
Define wall motion relative to adjacent cell zone?	yes
Apply a rotational velocity to this wall?	no
Velocity Magnitude (m/s)	0
X-Component of Wall Translation	1
Y-Component of Wall Translation	0
Z-Component of Wall Translation	0
Define wall velocity components?	no
X-Component of Wall Translation (m/s)	0
Y-Component of Wall Translation (m/s)	0
Z-Component of Wall Translation (m/s)	0
Internal Emissivity	1
External Emissivity	1
External Radiation Temperature (k)	300
Radiation BC Type	3
X-Component of Radiation Direction	1
Y-Component of Radiation Direction	0
Z-Component of Radiation Direction	0
Theta width of Beam (deg)	

report

9.9923854e-07
 Phi width of Beam (deg)
 9.9923854e-07

((constant . 0) (profile))

((constant . 0) (profile)))

	(1)
Apply Direct Irradiation Parallel to the Beam?	yes
Use Beam Direction from Solar Load Model Settings	no
Use Direct and Diffuse Irradiation from Solar Load Model Settings	no
Rotation Speed (rad/s)	0
X-Position of Rotation-Axis Origin (m)	0
Y-Position of Rotation-Axis Origin (m)	0
Z-Position of Rotation-Axis Origin (m)	0
X-Component of Rotation-Axis Direction	0
Y-Component of Rotation-Axis Direction	0
Z-Component of Rotation-Axis Direction	1
X-component of shear stress (pascal)	0
Y-component of shear stress (pascal)	0
Z-component of shear stress (pascal)	0
Fslip constant	0
Eslip constant	0
Surface tension gradient (n/m-k)	0
Specularity Coefficient	0

wall-part-pipe

Condition	Value
-----------	-------

Wall Thickness (m)	0
Heat Generation Rate (w/m3)	0
Material Name	
aluminum	
Thermal BC Type	1
Temperature (k)	300
Heat Flux (w/m2)	0

Convective Heat Transfer Coefficient (w/m2-k)	0
Free Stream Temperature (k)	300
Enable shell conduction?	no
Wall Motion	0
Shear Boundary Condition	0
Define wall motion relative to adjacent cell zone?	yes
Apply a rotational velocity to this wall?	no
Velocity Magnitude (m/s)	0
X-Component of Wall Translation	1
Y-Component of Wall Translation	0
Z-Component of Wall Translation	0
Define wall velocity components?	no
X-Component of Wall Translation (m/s)	0
Y-Component of Wall Translation (m/s)	0
Z-Component of Wall Translation (m/s)	0
Internal Emissivity	1
External Emissivity	1
External Radiation Temperature (k)	300
Radiation BC Type	3
X-Component of Radiation Direction	1
Y-Component of Radiation Direction	0
Z-Component of Radiation Direction	0
Theta width of Beam (deg)	
9.9923854e-07	
Phi width of Beam (deg)	
9.9923854e-07	
((constant . 0) (profile))	
((constant . 0) (profile))	(1)
Apply Direct Irradiation Parallel to the Beam?	yes
Use Beam Direction from Solar Load Model Settings	no
Use Direct and Diffuse Irradiation from Solar Load Model Settings	no
Rotation Speed (rad/s)	0
X-Position of Rotation-Axis Origin (m)	0

report	
Y-Position of Rotation-Axis Origin (m)	0
Z-Position of Rotation-Axis Origin (m)	0
X-Component of Rotation-Axis Direction	0
Y-Component of Rotation-Axis Direction	0
Z-Component of Rotation-Axis Direction	1
X-component of shear stress (pascal)	0
Y-component of shear stress (pascal)	0
Z-component of shear stress (pascal)	0
Fslip constant	0
Eslip constant	0
Surface tension gradient (n/m-k)	0
Specularity Coefficient	0
wall-part-inner_fluid-part-pipe	
Condition	Value

Wall Thickness (m)	0
Heat Generation Rate (w/m3)	0
Material Name	aluminum
Thermal BC Type	3
Temperature (k)	300
Heat Flux (w/m2)	0
Convective Heat Transfer Coefficient (w/m2-k)	0
Free Stream Temperature (k)	300
Enable shell conduction?	no
Wall Motion	0
Shear Boundary Condition	0
Define wall motion relative to adjacent cell zone?	yes
Apply a rotational velocity to this wall?	no
Velocity Magnitude (m/s)	0
X-component of wall Translation	1

	report	
Y-Component of wall Translation		0
Z-Component of wall Translation		0
Define wall velocity components?		no
X-Component of Wall Translation (m/s)		0
Y-Component of Wall Translation (m/s)		0
Z-Component of Wall Translation (m/s)		0
Internal Emissivity		1
External Emissivity		1
External Radiation Temperature (k)		300
Radiation BC Type		3
X-Component of Radiation Direction		1
Y-Component of Radiation Direction		0
Z-Component of Radiation Direction		0
Theta Width of Beam (deg)		
9.9923854e-07		
Phi width of Beam (deg)		
9.9923854e-07		
(((constant . 0) (profile)))		
(((constant . 0) (profile)))		
		(1)
Apply Direct Irradiation Parallel to the Beam?		yes
Use Beam Direction from Solar Load Model Settings		no
Use Direct and Diffuse Irradiation from Solar Load Model Settings		no
Rotation Speed (rad/s)		0
X-Position of Rotation-Axis Origin (m)		0
Y-Position of Rotation-Axis Origin (m)		0
Z-Position of Rotation-Axis Origin (m)		0
X-Component of Rotation-Axis Direction		0
Y-Component of Rotation-Axis Direction		0
Z-Component of Rotation-Axis Direction		1
X-component of shear stress (pascal)		0
Y-component of shear stress (pascal)		0
Z-component of shear stress (pascal)		0
Fslip constant		0

report

Eslip constant 0
 Surface tension gradient (n/m-k) 0
 Specularity Coefficient 0

inner_inlet

Condition	Value
Velocity Specification Method	2
Reference Frame	0
Velocity Magnitude (m/s)	4.4
Supersonic/Initial Gauge Pressure (pascal)	0
Coordinate System	0
X-Velocity (m/s)	0
Y-Velocity (m/s)	0
Z-Velocity (m/s)	0
X-Component of Flow Direction	1
Y-Component of Flow Direction	0
Z-Component of Flow Direction	0
X-Component of Axis Direction	1
Y-Component of Axis Direction	0
Z-Component of Axis Direction	0
X-Coordinate of Axis Origin (m)	0
Y-Coordinate of Axis Origin (m)	0
Z-Coordinate of Axis Origin (m)	0
Angular velocity (rad/s)	0
Temperature (k)	267.5
Turbulent Specification Method	0
Turbulent Kinetic Energy (m2/s2)	0.01
Turbulent Dissipation Rate (m2/s3)	0.1
Turbulent Intensity (%)	10
Turbulent Length Scale (m)	1
Hydraulic Diameter (m)	1
Turbulent Viscosity Ratio	10
External Black Body Temperature Method	0
Black Body Temperature (k)	300
Internal Emissivity	1
is zone used in mixing-plane model?	no

inner_outlet

Condition	Value
Gauge Pressure (pascal)	0
Backflow Total Temperature (k)	300
Backflow Direction Specification Method	1
Coordinate System	0
X-Component of Flow Direction	1
Y-Component of Flow Direction	0
Z-Component of Flow Direction	0
X-Component of Axis Direction	1
Y-Component of Axis Direction	0
Z-Component of Axis Direction	0
X-Coordinate of Axis Origin (m)	0
Y-Coordinate of Axis Origin (m)	0
Z-Coordinate of Axis Origin (m)	0
Turbulent Specification Method	0
Backflow Turbulent Kinetic Energy (m2/s2)	1
Backflow Turbulent Dissipation Rate (m2/s3)	1

```

report
Backflow Turbulent Intensity (%) 10
Backflow Turbulent Length Scale (m) 1
Backflow Hydraulic Diameter (m) 1
Backflow Turbulent Viscosity Ratio 10
External Black Body Temperature Method 0
Black Body Temperature (k) 300
Internal Emissivity 1
is zone used in mixing-plane model? no
Radial Equilibrium Pressure Distribution no
Specify Average Pressure Specification no
Specify targeted mass flow rate no
Targeted mass flow (kg/s) 1
Upper Limit of Absolute Pressure Value (pascal) 5000000
Lower Limit of Absolute Pressure Value (pascal) 1

```

symmetry_1-part-inner_fluid

```

Condition Value
-----

```

symmetry_1-part-pipe

```

Condition Value
-----

```

symmetry_1-part-outer_fluid

```

Condition Value
-----

```

symmetry_2-part-inner_fluid

```

Condition Value
-----

```

symmetry_2-part-pipe

```

Condition Value
-----

```

symmetry_2-part-outer_fluid

```

Condition Value
-----

```

wall

Condition	Value
wall Thickness (m)	0
Heat Generation Rate (w/m3)	0
Material Name	ice_1
Thermal BC Type	0
Temperature (k)	273
Heat Flux (w/m2)	0

report

Convective Heat Transfer Coefficient (w/m2-k)	0
Free Stream Temperature (k)	300
Enable shell conduction?	no
wall Motion	0
Shear Boundary Condition	0
Define wall motion relative to adjacent cell zone?	yes
Apply a rotational velocity to this wall?	no
Velocity Magnitude (m/s)	0
X-Component of wall Translation	1
Y-Component of wall Translation	0
Z-Component of wall Translation	0
Define wall velocity components?	no
X-Component of wall Translation (m/s)	0
Y-Component of wall Translation (m/s)	0
Z-Component of wall Translation (m/s)	0
Internal Emissivity	1
External Emissivity	1
External Radiation Temperature (k)	300
Radiation BC Type	3
X-Component of Radiation Direction	1
Y-Component of Radiation Direction	0
Z-Component of Radiation Direction	0
Theta Width of Beam (deg)	
9.9923854e-07	
Phi Width of Beam (deg)	
9.9923854e-07	
(((constant . 0) (profile)))	
(((constant . 0) (profile)))	(1)
Apply Direct Irradiation Parallel to the Beam?	no
Use Beam Direction from Solar Load Model Settings	no
Use Direct and Diffuse Irradiation from Solar Load Model Settings	no
Rotation Speed (rad/s)	0

	report	
X-Position of Rotation-Axis Origin (m)		0
Y-Position of Rotation-Axis Origin (m)		0
Z-Position of Rotation-Axis Origin (m)		0
X-Component of Rotation-Axis Direction		0
Y-Component of Rotation-Axis Direction		0
Z-Component of Rotation-Axis Direction		1
X-component of shear stress (pascal)		0
Y-component of shear stress (pascal)		0
Z-component of shear stress (pascal)		0
Fslip constant		0
Eslip constant		0
Surface tension gradient (n/m-k)		0
Specularity Coefficient		0

Solver Settings

Equations

Equation	Solved
Flow	yes
Turbulence	yes
Energy	yes
Discrete Ordinates	yes

Numerics

Numeric	Enabled
Absolute Velocity Formulation	yes

Relaxation

Variable	Relaxation Factor
Pressure	0.3
Density	1
Body Forces	1
Momentum	0.7
Turbulent Kinetic Energy	0.8
Turbulent Dissipation Rate	0.8
Turbulent Viscosity	1
Energy	1
Discrete Ordinates	1

Linear Solver

variable	Solver Type	Termination Criterion	Residual Reduction Tolerance
----------	-------------	-----------------------	------------------------------

report

Pressure	V-Cycle	0.1	
X-Momentum	Flexible	0.1	0.7
Y-Momentum	Flexible	0.1	0.7
Z-Momentum	Flexible	0.1	0.7
Turbulent Kinetic Energy	Flexible	0.1	0.7
Turbulent Dissipation Rate	Flexible	0.1	0.7
Energy	Flexible	0.1	0.7
Discrete Ordinates	Flexible	0.1	0.7

Pressure-Velocity Coupling

Parameter	Value
Type	SIMPLE

Discretization Scheme

variable	Scheme
Pressure	Standard
Momentum	Second Order Upwind
Turbulent Kinetic Energy	Second Order Upwind
Turbulent Dissipation Rate	Second Order Upwind
Energy	Second Order Upwind
Discrete Ordinates	First Order Upwind

Solution Limits

Quantity	Limit
Minimum Absolute Pressure	1
Maximum Absolute Pressure	5e+10
Minimum Temperature	1
Maximum Temperature	5000
Minimum Turb. Kinetic Energy	1e-14
Minimum Turb. Dissipation Rate	1e-20
Maximum Turb. Viscosity Ratio	100000

APPENDIX D

Pipe 0.0002 m thickness	1	2	3	4	5	6
mass-weighted average enthalpy (J/kg)						
inner_inlet	-74019.76	-74019.75	-74019.58	-74019.33	-74019.73	-74019.73
inner_outlet	-74012.18	-74009.27	-74009.52	-74007.24	-74002.15	-73996.27
difference	7.58	10.48	10.06	12.09	17.58	23.46
J/kg-m (quarter pipe)	37.9	52.4	50.3	60.45	87.9	117.3
J/kg-m (full pipe)	151.6	209.6	201.2	241.8	351.6	469.2
Pipe 0.0004 m thickness	1	2	3	4	5	6
mass-weighted average enthalpy (J/kg)						
inner_inlet	-74019.76	-74019.75	-74019.602	-74019.42	-74019.74	-74019.73
inner_outlet	-74013.13	-74011.54	-74011.203	-74009.65	-74006.59	-74005.29
difference	6.63	8.21	8.399	9.77	13.15	14.44
J/kg-m (quarter pipe)	33.15	41.05	41.995	48.85	65.75	72.2
J/kg-m (full pipe)	132.6	164.2	167.98	195.4	263	288.8

THIS PAGE INTENTIONALLY LEFT BLANK

APPENDIX E

Pipe 0.0002 m thickness	1	2	3	4	5	6
total heat transfer rate (W)						
inner_inlet	-28190.90608	-28190.90614	-28190.90621	-28105.24270	-28105.24278	-28105.24349
inner_outlet	28188.02189	28186.90937	28187.00132	28100.49146	28098.55725	28096.33527
net results	2.88419	3.99677	3.90489	4.75124	6.68553	8.90822
W/m (quarter pipe)	14.42095559	19.98385586	19.52443345	23.75621690	33.42766325	44.54110230
W/m (full pipe)	57.68382234	79.93542344	78.09773381	95.02486762	133.71065301	178.16440919
Energy (1 second, J)	57.68382234	79.93542344	78.09773381	95.02486762	133.71065301	178.16440919
m _{ice} produced (kg)	0.00017271	0.00023933	0.00023383	0.00028451	0.00040033	0.00053343
^^based on solidification rate of ice						
volume	1.88503E-07	2.61218E-07	2.55212E-07	3.10528E-07	4.36947E-07	5.82216E-07
^^based on density						
Pipe 0.0004 m thickness	1	2	3	4	5	6
total heat transfer rate (W)						
inner_inlet	-28190.906050	-28246.585924	-28246.585510	-28105.242668	-28105.242300	-28105.242464
inner_outlet	28188.369141	28243.442441	28243.321652	28101.407572	28100.246475	28099.730722
net results	2.53691	3.14348	3.26386	3.83510	4.99583	5.51174
W/m (quarter pipe)	12.68454113	15.71741158	16.31928808	19.17548190	24.97912600	27.55871181
W/m (full pipe)	50.73816452	62.86964633	65.27715232	76.70192759	99.91650399	110.23484724
Energy (1 second, J)	50.73816452	62.86964633	65.27715232	76.70192759	99.91650399	110.23484724
m _{ice} produced (kg)	0.00015191	0.00018823	0.00019544	0.00022965	0.00029915	0.00033004
^^based on solidification rate of ice						
volume	1.65805E-07	2.05449E-07	2.13316E-07	2.50651E-07	3.26513E-07	3.60232E-07
^^based on density						

THIS PAGE INTENTIONALLY LEFT BLANK

LIST OF REFERENCES

- [1] R. Repice et al. "Annual Energy Review 2011," U.S. Energy Information Admin., Washington, DC, Rep. EIA-0384, Sep. 2012.
- [2] J. Conti et al. "Annual Energy Outlook 2013 with Projections to 2040," U.S. Energy Information Admin., Washington, DC, Rep. EIA-0383, Apr. 2013.
- [3] Biofuels Issues and Trends. (2012, Oct.) U.S. Energy Information Admin., Washington D.C. [Online]. Available: <http://www.eia.gov/biofuels/issuestrends/pdf/bit.pdf>
- [4] B. Bierwagen et al. (2012, Jul.) Biofuels and the Environment. United States Environmental Protection Agency, Washington, DC. [Online]. Available: <http://www.epa.gov/ncea/biofuels/basicinfo.htm>
- [5] A. J. Salkind, A. G. Cannone and F. A. Trumbure, "Lead-acid Batteries," in *Handbook of Batteries*, 3rd Edn., D. Linden and T.B. Reddy, Eds. New York, NY: McGraw-Hill Professional, 2002, pp. 23.1-23.88.
- [6] "Electropaedia: Battery and Energy Technologies." [Online]. Available: <http://www.mpoweruk.com/chemistries.htm>, 2005
- [7] Department of Defense. (2013, Mar.) Fiscal Year 2011 Operational Energy Annual Report.[Online]. Available: <http://energy.defense.gov/FY2011OperationalEnergyAnnualReport.pdf>
- [8] Department of Defense. (2012, Mar.) Operational Energy Strategy: Implementation Plan. [Online]. Available: http://energy.defense.gov/Operational_Energy_Strategy_Implementation_Plan.pdf
- [9] Deloitte Development LLC. (2009) Energy Security: America's Best Defense. [Online]. Available: http://www.deloitte.com/assets/Dcom-UnitedStates/Local%20Assets/Documents/AD/us_ad_EnergySecurity052010.pdf
- [10] Assistant Secretary of Defense for Operational Energy, Plans & Programs. (2011, May) Energy for the Warfighter: Operational Energy Strategy. [Online]. Available: http://energy.defense.gov/OES_report_to_congress.pdf
- [11] M. Schwartz, K. Blakeley and R. O'Rourke (2012, Dec. 10) Department of Defense Energy Initiatives: Background and Issues for Congress. Congressional Research Service. [Online]. Available: <http://www.fas.org/sgp/crs/natsec/R42558.pdf>

- [12] S. Booth, J. Barnett, K. Burman, J. Hambrick and R. Westby, "Net Zero Energy Military Installations: A Guide to Assessment and Planning," National Renewable Energy Laboratory, Golden, CO, Tech. Rep. NREL/TP-7A2-48876, 2010.
- [13] "Energy, Environment and Climate Change: Power." [Online]. Available: <http://greenfleet.dodlive.mil/environment/land-based-efforts/solar-wind-and-geothermal-power/>
- [14] F. Sehar, "Impact of Ice Storage on Electrical Energy Consumption in Large and Medium-Sized Office Buildings in Different Climate Zones," M.S. thesis, Dept. Elect. Eng., Virginia Polytechnic Institute and State University, Arlington, VA, 2011.
- [15] M. Farahani and N. Saeidi, "Case Study of Design and Implementation of a Thermal Energy Storage System," in *First International Power and Energy Conference*, Putrajaya, 2006, pp.6-11.
- [16] P. Ihm, M. Krarti and G. P. Henze, "Development of a thermal energy storage model forEnergyPlus," *Energy and Buildings*, vol. 36, pp. 807-814, 2004.
- [17] H. C. Davis, "Wind-Electric Ice Making for Developing World Villages," M.S. thesis, Dept. of Mech. Eng., University of Colorado, Boulder, CO, 1994.
- [18] K. Taylor, "Method for VAWT Placement on a Complex Building Structure," M.S. thesis, Dept. of Mech. Eng., Naval Postgraduate School, Monterey, CA, 2013.
- [19] "Urban Green Energy." Urban Green Energy. [Online]. Available: urbangreenenergy.com
- [20] "CALMAC." CALMAC Manufacturing Corp. [Online]. Available: <http://www.calmac.com/>
- [21] U.S. Energy Information Administration. (2013, May 10). How dependent are we on foreign oil?. [Online]. Available: http://www.eia.gov/energy_in_brief/article/foreign_oil_dependence.cfm
- [22] U.S. Department of Energy. (2013, Jan. 17). The Inside of a Wind Turbine. [Online]. Available: http://www1.eere.energy.gov/wind/inside_a_wind_turbine.html
- [23] Pacific Gas and Electric Company. (1997, May). Thermal Energy Storage Strategies for Commerical HVAC Systems. [Online]. Available: <http://www.pge.com/includes/docs/pdfs/about/edusafety/training/pec/inforesource/thrmstor.pdf>

INITIAL DISTRIBUTION LIST

1. Defense Technical Information Center
Ft. Belvoir, Virginia
2. Dudley Knox Library
Naval Postgraduate School
Monterey, California